Bayesian Inference and Predictive Performance of Soil Respiration Models in the Presence of Model Discrepancy

Ahmed S. Elshall[1,2], Ming Ye[3,*], Guo-Yue Niu[4,5] and Greg A. Barron-Gafford[4,6]

[1] Department of Earth Sciences, University of Hawai'i Manoa, Honolulu, Hawaii, USA
[2] Water Resources Research Center, University of Hawai'i Manoa, Honolulu, Hawaii, USA
[3] Department of Scientific Computing, Florida State University, Tallahassee, Florida
[4] Biosphere 2, University of Arizona, Tucson, Arizona
[5] Department of Hydrology and Water Resources, University of Arizona, Tucson, Arizona
[6] School of Geography and Development, University of Arizona, Tucson, Arizona

*Corresponding Author: Ming Ye, Telephone: (850) 644-4587, Email: mye@fsu.edu

Submitted for publication in Geoscientific Model Development

March, 2019

Key Points

(1) Bayesian inference and prediction are useful to evaluate multiple soil respiration models with different levels of model complexity.

(2) Data models used in Bayesian inference have substantial impacts on model parameter distributions and subsequently model predictions.

(3) Using exponential power distribution and considering heteroscedasticity in data models improves Bayesian inference and prediction.

Keywords: Soil respiration, Bayesian, likelihood function, data model, autocorrelation, heteroscedasticity, skew exponential power distribution, cross-validation, relative model score

Abstract

Bayesian inference of microbial soil respiration models is often based on the assumptions that the residuals are independent (i.e. no temporal or spatial correlation), identically distributed (i.e. Gaussian noise) and with constant variance (i.e. homoscedastic). In the presence of model discrepancy, since no model is perfect, this study shows that these assumptions are generally invalid in soil respiration modeling such that residuals have high temporal correlation, an increasing variance with increasing magnitude of CO_2 efflux, and non-Gaussian distribution. Relaxing these three assumptions stepwise results in eight data models. Data models are the basis of formulating likelihood functions of Bayesian inference. This study presents a systematic and comprehensive investigation of the impacts data model selection on Bayesian inference and predictive performance. We use three mechanistic soil respiration models with different levels of model fidelity (i.e. model discrepancy) with respect to number of carbon pools and explicit representations of soil moisture controls on carbon degradation, and accordingly have different levels of model complexity with respect to the number of model parameters. The study shows data models have substantial impacts on Bayesian inference and predictive performance of the soil respiration models such that: (i) the level of complexity of the best model is generally justified by the cross-validation results for different data models; (ii) not accounting for heteroscedasticity and autocorrelation might not necessarily result in biased parameter estimates or predictions, but will definitely underestimate uncertainty; (iii) using a non-Gaussian data model improves the parameter estimates and the predictive performance; and (iv) separate accounting for autocorrelation or joint inversion of correlation and heteroscedasticity can be problematic and requires special treatment. Although the conclusions of this study are empirical, the analysis may provide insights for selecting appropriate data models for soil respiration modeling.

1 Introduction

Developing accurate soil respiration models is important for realistic projection of global carbon [C] cycle, as global soils store 2,300Pg carbon, an amount more than 3 times that of the atmosphere (Schmidt et al., 2011) and release 60–75 Pg C/yr, about 7 times more CO_2 to the atmosphere than all human-caused emissions (Le Quéré et al., 2014). The major work on soil respiration modeling has been focused on advancing knowledge about model inputs and calibration data (e.g. Janssens et al., 2003; Peters et al., 2007; Scott et al., 2009; Barron-Gafford et al., 2011; Hilton et al., 2014) and on developing more advanced models for better representing soil microbial processes (e.g. Schimel and Weintraub, 2003; Allison et al., 2010; Davidson et al., 2011; Wieder et al., 2013, 2015; Xu et al., 2014; Zhang et al., 2014) . Integration of data and models is indispensable for improving predictability of the terrestrial carbon cycle, and statistical modeling is a vital tool for the model-data integration (Luo et al., 2011, 2014; Wieder et al., 2015). In addition, use of state-of-the-art statistical methods is necessary to accurately quantify uncertainty in parameters and structures of soil respiration models for improvement and practical uses of the models (Katz et al., 2013). A data model that is also known as a residuals model or an error model is used to characterize residuals (i.e., the difference between data and corresponding model simulations). While a large number of data models have been used (e.g. Elshall et al., 2018; Scholz et al., 2018) to our knowledge comprehensive and systematic evaluation of data models for soil respiration modeling has not been reported in literature.

The goal of this study is to evaluate the impacts of data models on Bayesian inference and predictive performance of three mechanistic soil respiration models, and use these findings to make broader recommendations. The three models were developed by Zhang et al. (2014) to simulate the Birch effect (the peak soil microbial respiration pulses in response to episodic rainfall

117 pulses) at a site scale and a short temporal scale, which are important for gaining mechanistic
118 understanding of CO_2 efflux production (Högberg and Read, 2006; Vargas et al., 2011). Zhang et
119 al. (2014) developed a total five models, including an existing four-carbon pool model and four
120 new models with additional carbon pools and/or explicit representations of soil moisture controls
121 on carbon degradation and microbial uptake rates. The models Zhang et al. (2014) were calibrated,
122 and Bayesian model selection was used to select the best model. However, this effort was based
123 on a single data model. It is unknown whether the best model still remains the best (in terms of
124 reproducing the both calibration data and the cross-validation data) if a different data model is
125 used. In addition, since predictive performance of the models was not evaluated in Zhang et al.
126 (2014), it is unknown whether the best model will give the best predictions. These two questions
127 are addressed in this study by considering eight data models and by evaluating predictive
128 performance in a manner of cross-validation. The top two models (also the two most high fidelity
129 models) ranked by Zhang et al. (2014) are considered in this study, and the worst model (also the
130 low fidelity model) is also considered in this study for comparison. We use the terms model fidelity
131 and model discrepancy interchangeably. Model fidelity refers to the degree of realism of
132 representing our scientific knowledge with respect to the real world system. That is a high fidelity
133 model has less discrepancy. Conducting Bayesian inference and evaluating predictive performance
134 for the three models with different degrees of fidelity provides more insights than for a single
135 model.

136 Bayesian inference in general uses the Bayes' theorem to update the distributions of model
137 parameters to posterior parameter distributions given a likelihood function. The mathematical
138 formulation of the (formal and informal) likelihood function requires a probabilistic data model
139 that however is intrinsically unknown due to unknown errors in all model components such as

observation data, model structures, parameters, and driving forces. Bayesian inference of soil respiration models often adopts the assumption of independent, normally distributed and homoscedastic residuals (e.g. Ahrens et al., 2014; Bagnara et al., 2015, 2018; Barr et al., 2013; Barron-gafford et al., 2014; Braakhekke et al., 2014; Braswell et al., 2015; Correia et al., 2012; Du et al., 2015, 2017; Hararuk et al., 2014; Hashimoto et al., 2011; He et al., 2018; Klemedtsson et al., 2008; Menichetti et al., 2016; Raich et al., 2002; Ren et al., 2013; Richardson and Hollinger, 2005; Steinacher and Joos, 2016; Tucker et al., 2014; Tuomi et al., 2008; Xu et al., 2006; Yeluripati et al., 2009; Yuan et al., 2012, 2016; Zhang et al., 2014; Zhou et al., 2010). These assumptions are conveniently adopted since the requirement of using an unknown probability model in Bayesian statistics is called "a basic dilemma" by Box and Tiao (1992). Postulating the data models is always based on assumptions about residual statistics, and the most widely used assumptions are paired as follows: (i) independent vs. correlated residuals, (ii) homoscedastic vs. heteroscedastic residuals, and (iii) Gaussian vs. non-Gaussian residuals. For soil respiration modeling few studies have relaxed the non-correlation assumption(e.g. Cable et al., 2008, 2011; Li et al., 2016b), the homoscedasticity assumption(e.g. Berryman et al., 2018; Elshall et al., 2018; Ogle et al., 2016; Tucker et al., 2013), and the non-Gaussian and homoscedasticity assumptions (e.g. Elshall et al., 2018; Ishikura et al., 2017; Kim et al., 2014). A recent study (Scholz et al., 2018) relaxed these three assumptions using the generalized likelihood function (Schoups and Vrugt, 2010). However, few studies have focused on investigating appropriateness and impact of these assumptions for soil respiration modeling, by relaxing the independent residuals assumption (Ricciuto et al., 2011) and the Gaussian residuals assumption (Ricciuto et al., 2011; van Wijk et al., 2008). By relaxing these three assumptions stepwise resulting in eight data models, to our knowledge this is the first study that systematically evaluates the impact of data model selection on Bayesian inference and

predictive performance of soil respiration modeling. In addition, to our knowledge this is the first soil respiration modeling study that investigates the impact of data models in relation to model fidelity.

Relaxing these three assumption results in eight data models, which are shown in details in Section 2. For example, combining the assumptions of independent, homoscedastic, and Gaussian residuals leads to the standard least squares data model. This model is the simplest one among the eight data models, since it requires only one parameter, i.e., the constant variance of the Gaussian distribution. Note that there is a difference between the soil respiration model parameters and data model parameters. They technically can be estimated together, but one arises from assumptions about soil respiration processes, and the other assumptions about the residuals. Relaxing the homoscedastic assumption to heteroscedastic gives the weighted least squares data model. It is more complex because it has extra parameters to account for multiple variances for multiple data. Whenever one or combinations of the three assumptions (independence, homoscedasticity, and normality) are relaxed, the resulting data models become more complex and require more parameters. Such systematic evaluation of data models (McInerney et al., 2017; Smith et al. 2010b, 2015) is necessary to evaluate appropriateness of residuals assumptions and their impacts on Bayesian inference.

The assumptions of heteroscedastic, correlated, and non-Gaussian residuals are accounted for using the method of Schoups and Vrugt (2010) in the following procedure: (i) the correlation is removed from the residuals by using an autoregressive model; (ii) the resulting residuals are normalized by a linear model of variance; and (iii) the normalized residuals are characterized by using the skew exponential power distribution. The data model parameters (i.e., coefficients of the autoregressive model, the linear variance model, and the skew exponential power distribution) are

not specified by users, but estimated together with soil respiration model parameters during the Bayesian inference. The skew exponential power distribution is general in that by adjusting the values of its kurtosis and skewness parameters the distribution can produce other distributions such as the Laplace distribution (van Wijk et al., 2008; Ricciuto et al., 2011) and other distributions through using an exponential model with different kurtosis parameters (Tang and Zhuang, 2009). It is worth pointing out that there exist other methods to account for the three assumptions. Evin et al. (2013) suggested accounting for residual heteroscedasticity before accounting for residual autocorrelation. Lu et al. (2013) developed an iterative two-stage procedure to separately estimate physical model parameters and data model parameters. Evin et al. (2014) developed a similar procedure to first estimate model parameters and then estimate heteroscedasticity and autocorrelation parameters. While this study uses the method of Schoups and Vrugt (2010), exploring other methods is warranted in future studies.

After investigating the impacts of the data models on Bayesian inference, this study evaluates the impacts of the data models on predictive performance of the three soil respiration models. Using random samples generated during the Bayesian inference, a prediction ensemble is produced for each soil respiration model. The ensemble is used to evaluate predictive performance of the models in a stochastic sense by estimating to what extent the models can predict future events. The evaluation in this study is done in a cross-validation manner by splitting the dataset of CO_2 efflux into two parts for Bayesian inference and cross-validation, respectively. The evaluation of predictive performance is important because different data models may give different parameter distributions and accordingly different predictive performance. For example, the study of van Wijk et al. (2008) concluded that the choice of the residual function is crucial to achieve accurate model prediction and parameter estimation. Shi et al. (2014) showed that the posterior parameter

distributions and predictive performance given by two data models (weighted least square and skew exponential power distribution after removing heteroscedasticity and autocorrelation) are dramatically different, and a definitive conclusion was drawn that one data model is better than the other. The evaluation of predictive analysis is conducted for the following two cases: (1) the prediction ensemble is generated by random samples of the soil respiration models only (i.e. credible interval), and (2) the prediction ensemble is generated by random samples of not only the soil respiration models but also the data models (i.e. predictive interval). The two cases lead to different conclusions about the predictive performance. It is expected that the evaluation of predictive performance conducted in this study can help select the most appropriate data model to achieve optimal model predictions.

The remainder of the paper is organized as follows. Section 2 starts with a description of the evolving data models and their corresponding likelihood functions used in Bayesian inference, followed by a brief summary of the three soil respiration models. The results of Bayesian inference are discussed in Section 3 and Section 4, addressing the data model implications on parameter estimation and predictive performance, respectively. Section 5 summarizes the key findings and limitations of this study, and provides recommendations for approaching data model selection.

2 Methodology

This section starts with a description of the eight data models that account for the three pairs of assumptions about residuals in a stepwise manner in Section 2.1. The data models are used to build the likelihood functions used in Section 2.2 for Bayesian inference. The three soil respiration models and observations of CO_2 efflux are described in Sections 2.3 and 2.4, respectively. Metrics for evaluating predictive performance are presented in Section 2.5.

2.1 Data models

This study considers eight evolving data models starting from a data model that assumes independent, homoscedastic, and Gaussian residuals to a data model that relaxes all the three assumptions. The eight data models are based on the generic normalized residual,

$$a_t = \frac{\varepsilon_t}{\sigma_t} \qquad a_t \sim X\,, \tag{1}$$

where $\varepsilon_t = d_t - Y_t$ is the residual (the difference between data d_t and its corresponding model simulation Y_t) at time or location t; σ_t is the standard deviation of the residual; and X is the probability density function (PDF) of a_t. The eight data models are formulated with different forms of ε_t, σ_t, and X. The standard least square (SLS) data model is

$$a_t = \frac{\varepsilon_t}{\sigma_0} \qquad a_t \sim N(0,1)\,, \tag{2}$$

where $\sigma_t = \sigma_0$ is a constant for all the data (i.e., homoscedasticity), and X is the standard normal distribution, $N(0,1)$. The unknown parameter σ_0 is estimated jointly with unknown physical model parameters. If σ_t is not a constant (i.e., heteroscedastic), SLS becomes the weighted least squared (WLS) data model. While heteroscedasticity can be accounted for through residuals transformation (e.g. Thiemann et al., 200; Smith et al., 2010b) or other similar approaches (Gragne et al., 2015) a linear heteroscedastic model $\sigma_t = \sigma_0 + \sigma_1 Y_t$ is assumed following other studies (Thyer et al., 2009; Schoups and Vrugt, 2010; Evin et al., 2013, 2014). With the linear model, there is no need to estimate σ_t for each data. Instead, σ_t is calculated by estimating only two parameters, σ_0 and σ_1. The WSL data model is written as

$$a_t = \frac{\varepsilon_t}{\sigma_0 + \sigma_1 Y_t} \qquad a_t \sim N(0,1)\,. \tag{3}$$

The two unknown parameters σ_0 and σ_1 are estimated jointly with unknown physical model parameters. The linear model assigns smaller weight to the data with larger simulation, Y_t. If the simulation is small and $\sigma_0 \gg \sigma_1 Y_t$, the weight becomes constant for all data. Both SLS and WLS assume that a_t is independently and identically distributed.

It is not uncommon that residuals are correlated in space and time, due to propagation of measurement errors (Tiedeman and Green, 2013) and model structure errors (Evin et al., 2014; Kavetski et al., 2013; Lu et al., 2013). The temporal correlation that occurs in the numerical example of this study can be accounted for using a *p*-order autoregressive model. This leads to the data model of standard least square with autocorrelation (SLS-AC),

$$a_t = \frac{\varepsilon_t - \sum_{i=1}^{p} \phi_i \varepsilon_{t-i}}{\sigma_0} \qquad a_t \sim N(0,1) \tag{4}$$

where *p* is the order of autocorrelation, and ϕ_i is an autocorrelation coefficient. The unknown ϕ_i and σ_0 are estimated together with unknown model parameters. By extending the concept of correlated residuals to WLS leads to the weight least square with autocorrelation (WLS-AC),

$$a_t = \frac{\varepsilon_t - \sum_{i=1}^{p} \phi_i \varepsilon_{t-1}}{\sigma_0 + \sigma_1 Y_t} \qquad a_t \sim N(0,1) \tag{5}$$

The unknown parameters of σ_0, σ_1, and ϕ_i are estimated jointly with physical model parameters. Equations (2) – (5) assume that the residuals are Gaussian.

The next four data models are similar to the previous four models except that the standard normal distribution of a_t is replaced by the skew exponential power distribution, $SEP(0,1,\xi,\beta)$, (Schoups and Vrugt, 2010)

$$p(a_t \mid \xi,\beta) = \frac{2\sigma_\xi}{\xi+\xi^{-1}}\omega_\beta \exp\left[-c_\beta \left|a_{\xi,t}\right|^{2/(1+\beta)}\right], \quad (6)$$

where zero is mean, one is standard deviation, ξ is skewness, β is kurtosis,

$a_{\xi,t} = (\mu_\xi + \sigma_\xi a_t)\Big/\xi^{sign(\mu_\xi+\sigma_\xi a_t)}$, $\mu_\xi = M(\xi - \xi^{-1})$, $\omega_\beta = \frac{\Gamma^{1/2}[3(1+\beta)/2]}{(1+\beta)\Gamma^{3/2}[(1+\beta)/2]}$,

$\sigma_\xi = \sqrt{(1-M^2)(\zeta^2+\zeta^{-2})+2M^2-1}$, $M = \frac{\Gamma[1+\beta]}{\Gamma^{1/2}[3(1+\beta)/2]\Gamma^{1/2}[(1+\beta)/2]}$, and

$c_\beta = \left(\frac{\Gamma[3(1+\beta)/2]}{\Gamma[(1+\beta)/2]}\right)^{1/(1+\beta)}$ are derived variables of β and ξ, and $\Gamma[.]$ is the gamma function. The kurtosis parameter $\{\beta \in \mathbb{R}: -1 \le \beta \le 1\}$ determines the peakness of the pdf such that the β values of -1, 0, and 1 give uniform, Gaussian and Laplace distributions, respectively. The skewness parameter $\{\xi \in \mathbb{R}: 0.1 \le \xi \le 10\}$ determines the skewness of the pdf such that the ξ values of 0.1, 1, and 10 give positively skewed, symmetric, and negatively skewed distributions, respectively. Setting $\beta = 0$ and $\xi = 1$ leads to $\mu_\xi = 0$, $\sigma_\xi = 1$, $\omega_\beta = 1/\sqrt{2\pi}$, $c_\beta = 1/2$ and $a_{\xi,t} = a_t$, and the skew exponential power distribution $SEP(0,1,\xi=1,\beta=0)$ becomes the standard normal distribution,

$$p(a_t \mid \xi=1,\beta=0) = \frac{1}{\sqrt{2\pi}}\exp\left[-\frac{1}{2}(a_t)^2\right]. \quad (7)$$

which is the data model of SLS in equation (2).

Replacing $a_t \sim N(0,1)$ with $a_t \sim SEP(0,1,\xi,\beta)$ in equations (2) – (5) leads to the data models SEP, WSEP, SEP-AC, and WSEP-AC as follows,

$$a_t = \frac{\varepsilon_t}{\sigma_0} \qquad a_t \sim SEP(0,1,\xi,\beta) \quad (8)$$

$$a_t = \frac{\varepsilon_t}{\sigma_0 + \sigma_1 Y_t} \qquad a_t \sim SEP(0,1,\xi,\beta)\,. \tag{9}$$

$$a_t = \frac{\varepsilon_t - \sum_{i=1}^{p} \phi_i \varepsilon_{t-1}}{\sigma_0} \qquad a_t \sim SEP(0,1,\xi,\beta) \tag{10}$$

$$a_t = \frac{\varepsilon_t - \sum_{i=1}^{p} \phi_i \varepsilon_{t-1}}{\sigma_0 + \sigma_1 Y_t} \qquad a_t \sim SEP(0,1,\xi,\beta) \tag{11}$$

In comparison with the Gaussian data models, the SEP-based data models have two more parameters (ξ and β) to be estimated jointly with physical model parameters. WSEP-AC data model, which is known as the generalized likelihood function, is the most commonly used SEP-based data model (e.g. Vrugt and Ter Braak, 2011; Hublart et al., 2016; Scholz et al., 2018). A summary table of the eight data models with corresponding parameters is provided in the supplementary materials.

2.2 Bayesian inference and likelihood functions

Consider a Bayesian inference problem for a nonlinear model, *f*, used to simulate state variables (e.g., CO_2 efflux), $\boldsymbol{d} = \boldsymbol{Y}(\boldsymbol{\theta}) + \boldsymbol{e}$, where $\boldsymbol{d}$ is a vector of data, $\boldsymbol{\theta}$ is a vector of model parameters, and $\boldsymbol{e}$ is a vector of residuals that may include errors in data, model parameters, and model structures. The goal of Bayesian inference is to estimate the posterior distributions, $p(\boldsymbol{\theta}|\boldsymbol{d})$, of model parameters, $\boldsymbol{\theta}$, given data, $\boldsymbol{d}$, using Bayes' theorem (Box and Tiao, 1992)

$$p(\boldsymbol{\theta}\,|\,\boldsymbol{d}) = \frac{p(\boldsymbol{d}\,|\,\boldsymbol{\theta})\,p(\boldsymbol{\theta})}{\int p(\boldsymbol{d}\,|\,\boldsymbol{\theta})\,p(\boldsymbol{\theta})\,d\boldsymbol{\theta}} \tag{12}$$

where $p(\boldsymbol{\theta})$ is the prior distribution, and $p(\boldsymbol{d}|\boldsymbol{\theta})$ is the likelihood function to measure goodness-of-fit between model simulations, $\boldsymbol{Y}(\boldsymbol{\theta})$, and data, $\boldsymbol{d}$. The prior distribution can be obtained from data of previous studies (e.g. Elshall and Tsai, 2014) or expert judgment. When prior information is

lacking, a common practice is to assume uniform distributions with relatively large parameter ranges so that the prior distributions do not affect the estimation of posterior distributions.

The data models above can be used to construct the likelihood functions. For the Gaussian data models given in equations (2) – (5), the corresponding Gaussian likelihood functions are straightforward, and an example is equation (7). For the SEP data models, the corresponding likelihood that is called generalized likelihood function is (Schoups and Vrugt, 2010)

$$p(\boldsymbol{d}\,|\,\boldsymbol{\theta}) = p(\boldsymbol{\varepsilon}_t\,|\,\boldsymbol{\theta}) = \prod_{t=1}^{n} \sigma_t^{-1} \frac{2\sigma_\xi}{\xi+\xi^{-1}} \omega_\beta \exp\left(-c_\beta \left|a_{\xi,t}\right|^{2/(1+\beta)}\right). \tag{13}$$

where n is the dimension of $\boldsymbol{d}$. The Gaussian likelihood functions are special case of the generalized likelihood functions. For example, by setting $\beta = 0$, $\xi = 1$, $\phi_i = 0$, $\sigma_t = \sigma_0$, $\sigma_\xi = 1$, $\mu_\xi = 0$, $\omega_\beta = 1/\sqrt{2\pi}$, $c_\beta = 1/2$, and $a_{\xi,t} = a_t$, equation (13) becomes the likelihood function corresponding to the SLS data model. Replacing $\sigma_t = \sigma_0$ by $\sigma_t = \sigma_0 + \sigma_1 E_t$, equation (13) becomes the likelihood function of the WLS data model.

In this study, the posterior distributions of the data model parameters are jointly estimated with the soil respiration model parameters using the MT-DREAM$_{(ZS)}$ code (Laloy and Vrugt, 2012). MT-DREAM$_{(ZS)}$ implements a Markov chain Monte Carlo (MCMC) algorithm by running multiple Markov chains in parallel with adaptive proposal distribution, multiple-try sampling, and sampling from an archive of past states. These state-of-the-art features assist in overcoming common challenges in the sampling landscape such as multimodality, ill-conditioning, and high dimensionality, and thus allow for accurate exploration of the targeted distributions.

2.3 Soil respiration models

Zhang et al. (2014) studied the Birch effect (the peak soil microbial respiration pulses in response to episodic rainfall pulses), and developed five models, evolving from an existing four-

carbon pool model to models with additional carbon pools and/or explicit representations of soil moisture controls on carbon degradation and microbial uptake rates. Three of the five models are used in this study, and they are dented as 4C, 5C, and 6C. Note that model 4C is model 4C_NOSM of Zhang et al. (2014), not model 4C. Figure 1 is the diagram of model 6C, the most complex one among the five models. The simplest one, model 4C, has four carbon pools, i.e., soil organic carbon (SOC), dissolved organic carbon (DOC), microbial biomass (MIC), and enzymes (ENZ), and does not consider the soil moisture control on carbon degradation and microbial uptake rates. Models 5C and 6C has an explicit representation of soil moisture controls on the rates. Based on the dual Arrhenius and Michaelis–Menten kinetics model, the original SOC degradation rate, V_{decom}, is (Davidson et al., 2011; Davidson and Janssens, 2006)

$$V_{decom} = V_{\max} C_{ENZ} \frac{C_{SOC}}{K_m + C_{SOC}} \tag{14}$$

where $V_{\max}$ [s^{-1}] is the maximum SOC degradation rate per unit enzyme when the substrates is not limiting, C_{ENZ} [gCm^{-3}] is enzyme pool size, C_{SOC} [gCm^{-3}] is SOC pool size, and K_m is the half-saturation for SOC. The original microbial uptake rate, V_{uptake}, is (Davidson et al., 2011; Davidson and Janssens, 2006)

$$V_{uptake} = V_{\max\_up} C_{MIC} \frac{C_{DOC}}{K_{m\_up} + C_{DOC}} \frac{C_{O2}}{K_{m\_upO2} + C_{O2}}, \tag{15}$$

where $V_{\max\_up}$ [s^{-1}] is the maximum DOC uptake rate when the substrates is not limiting, C_{MIC} [gCm^{-3}] is the microbial biomass pool size, C_{DOC} [gCm^{-3}] is the DOC pool size, C_{O2} [m^3m^{-3}] is the gas concentration of O_2 in the soil pore, and K_{m_up} [gCm^{-3}] and K_{m_upO2} [m^3m^{-3}] are the corresponding half-saturation constants for DOC and O_2, respectively. With the explicit representation of soil moisture control, the two rates become (Zhang et al., 2014)

$$V_{decom} = V_{\max} C_{ENZ} \frac{C_{SOC}}{K_m + C_{SOC}} \left(\frac{\theta}{\theta_s} \right) \quad (16)$$

$$V_{uptake} = V_{\max\_up} C_{MIC} \frac{C_{DOC}}{K_{m\_up} + C_{DOC}} \frac{C_{O2}}{K_{m\_upO2} + C_{O2}} \left(\frac{\theta}{\theta_s} \right) \quad (17)$$

where θ [-] is the volumetric soil moisture, and θ_s [-] is the porosity.

In addition to using the new rate equations, models 5C and 6C have more carbon pools. In model 5C, DOC is split into two sub-pools for wet zone and dry zone of soil pores, and only the wet DOC is used by MIC, as shown in Figure 1. The moisture-controlled microbial uptake rate becomes

$$V_{uptake} = V_{\max\_up} C_{MIC} \frac{C_{DOC\_w}}{K_{m\_up} + C_{DOC\_w}} \frac{C_{O2}}{K_{m\_upO2} + C_{O2}} \left(\frac{\theta}{\theta_s} \right). \quad (18)$$

where C_{DOC_w} [gCm^{-3}] is the DOC pool size in the wet soil pores. Model 6C is more complex in that ENZ is further split into two sub-pools for wet and dry pores, and both the wet and dry ENZ are subject to degradation, as shown in Figure 1. The moisture-controlled SOC degradation rate becomes

$$V_{decom} = V_{\max} C_{ENZ\_W} \frac{C_{SOC}}{K_m + C_{SOC}} \left(\frac{\theta}{\theta_s} \right) \quad (19)$$

for the wet ENZ and

$$V_{decom} = V_{\max} C_{ENZ\_D} \frac{C_{SOC}}{K_m + C_{SOC}} \left(1 - \frac{\theta}{\theta_s} \right) \varepsilon_D \quad (20)$$

for the dry ENZ, where C_{ENZ_W} [gCm^{-3}] is the wet soil pores enzyme pool size, C_{ENZ_D} [gCm^{-3}] is the enzyme pool size in the dry soil pores, and ε_D is the catalysis efficiency of the dry zone enzyme.

Due to considering the moisture control and adding more soil pools, model 5C is expected to be significantly better than model 4C for simulating the Birch effect. Since the accumulated ENZ in dry soil is secondary, model 6C is expected to be slightly better than model 5C. In terms of model structural error, model 4C has the largest model structure error, model 5C has significantly less model structure error, and model 6C has the smallest model structural error. As shown below, the degree of model structural error is reflected in the process of Bayesian inference and verified by the cross-validation.

2.4 Observations and parameter estimation

Figure 2 plots the time series of 17,016 observations of soil moister and CO_2 efflux used in this study. The observations were obtained during the entire year of 2007, covering a long period of dry season prior to monsoon and episodic rainfall events during monsoon. The first two third of this dataset is used for the Bayesian inference, and the last one third is used for cross-validation. The inference and cross-validation periods have both dry and wet periods, as shown in Figure 2. The observation site is located within the Santa Rita Experimental Range (SRER, 31.8214°N, 110.8661°W, elevation 1,116 m) outside of Tucson, Arizona (Barron-Gafford et al., 2011; Scott et al., 2009). This savanna site was covered by 22% of perennial grass, forbs and subshrubs and 35% of mesquite. The soils are uniformly Comoro loamy sand (77.6% sand, 11.0% clay, and 11.4% silt). The half-hourly atmospheric forcing data were collected from measurements through an eddy covariance tower (Scott et al., 2009). This includes downward shortwave, longwave, precipitation, wind, air temperature, humidity, and pressure. Volumetric CO_2 concentration was measured at half-hourly interval through compact probes. The CO_2 efflux was estimated from the gradient of CO_2 concentration measured at two depths of 2 cm and 10 cm through Fick's first law

of diffusion, and the estimates were validated against measurements from a portable CO_2 gas analyzer.

The parameters estimated in this study include the parameters of the soil respiration models (4C – 6C) and the parameters of the data models described in Section 2.1. The estimated parameters of models 4C and 5C include the microbial carbon use efficiency (CUE) [g/g], enzyme production rate, k_e [g/m^{3}s], microbial turnover rate, τ_m [1/s], and enzyme turnover rate τ_e [1/s]. Uniform distributions are used as the prior in the Bayesian inference, and the ranges of the four parameters are 0.2 – 1.00, 1×10^{-12} – 1×10^{-7}, 1×10^{-12} – 1×10^{-5} and 1×10^{-11} – 1×10^{-6}, respectively. The values of other parameters are fixed at the values used in Allison et al. (2010). Model 6C has two more parameters, and they are the catalysis efficiency ε_D [-] and the turnover rate of the dry-zone enzymes τ_{en} [1/s]. The prior of the two parameters are uniform distributions with the ranges of 0.2 – 0.8 and 1×10^{-12} – 1×10^{-8}, respectively.

The DREAM-based MCMC simulation is conducted for a total of 24 cases, the combinations of eight data models and three soil respiration models. For each case, the parameter distributions are obtained after drawing a total of 5×10^5 samples using five Markov chains. The Gelman and Rubin (1992) R-statistic is used for convergence diagnostic, and it approaches one in less than 4×10^4 samples. The initial 50% of the samples are discarded during the burn-in period.

2.5 Metrics for evaluating predictive performance

Three criteria are used to evaluate the predictive performance of the soil respiration models and data models, and they are central mean tendency, dispersion, and reliability. Each criterion is measured by a single metric. In addition, a newly defined metric is also used for simultaneously measuring the three criteria. The central mean tendency is measured in this study using the Nash-Sutcliffe model efficiency (NSME) coefficient (Nash and Sutcliffe, 1970),

$$NSME = 1 - \sum_{i=1}^{n} (d_i - \overline{\mathbf{Y}_i})^2 \Big/ \sum_{i=1}^{n} (d_i - \overline{\mathbf{d}})^2 , \quad (21)$$

where n is the number of cross-validation data, d_i is the i-th data, $\overline{\mathbf{d}}$ is the mean of the data, and $\overline{\mathbf{Y}_i}$ is the mean of the prediction ensemble, $\boldsymbol{Y}_i$, for d_i. NSME ranges from -∞ to 1, with $NSME = 1$ corresponding to a perfect match between data and mean prediction, i.e., the ensemble is centered on the data. $NSME = 0$ indicates that the model predictions are as only accurate as the mean of the data, while an efficiency $NSME < 1$ indicates that the mean of data is a better prediction than the mean prediction.

In addition to the central mean tendency, it is also desirable that the ensemble is precise with small dispersion and reliable to cover all the data. This study uses a nonparametric metric for dispersion, and it is the sharpness of a prediction interval (e.g. Smith et al., 2010a)

$$Sharpness = 1/n \sum_{i=1}^{n} \left[Max(\mathbf{Y}_i) - \mathrm{Min}(\mathbf{Y}_i) \right] \quad (22)$$

where X_i is the prediction ensemble within the 95% prediction interval (the Bayesian credible interval, not the confidence interval used in nonlinear regression (Lu et al., 2013). Smaller values of sharpness indicate better prediction precision. Reliability is measured using predictive coverage. (e.g. Hoeting et al., 1999), which is the percentages of data contained in the prediction interval. Larger predictive coverage values are preferred.

To account for the trade-off between the three metrics,(Elshall et al., 2018b) defined relative model score (RMS) that simultaneously measure all the three criteria. Scoring rules are commonly used in hydrology to assess predictive performance (e.g. Weijs et al., 2010; Westerberg et al., 2011). RMS is used in this study to measure the relative predictive performance of the combinations of soil respiration models and data models. For combination M_j, RMS is defined as

$$RMS(M_j) = \sum_{i=1}^{n} \frac{p(d_i \mid \mathbf{Y}_{ij}, M_j)}{\sum_{j=1}^{m} p(d_i \mid \mathbf{Y}_{ij}, M_j)} \times 100 \quad (23)$$

where m is the number of combinations; and the ensemble prediction $\boldsymbol{Y}_{ij}$ is similar to $\boldsymbol{Y}_i$ above where is i index over time and specific to the j-th combination. The density function $p(d_i|\boldsymbol{Y}_{ij})$ can be evaluated by first obtaining the density function $p(\boldsymbol{Y}_{ij})$ of the ensemble prediction $\boldsymbol{Y}_{ij}$ (e.g., by using the kernel density function) and then evaluating $p(d_i|\boldsymbol{Y}_{ij})$ using interpolation methods based on the intersection of $\boldsymbol{Y}_{ij}$ and d_i. This evaluation is based purely on the model predictions, and does not involve any assumptions on the models, their parameters, and likelihood functions. Larger RMS values indicate better overall predictive performance. A figure of our workflow scheme is presented in the supplementary materials.

3 Results of Bayesian Inverse Modeling

This section analyzes the residuals of the best realization (with the highest likelihood value) of the MCMC simulation to understand whether the assumptions of the eight data models hold. The impacts of the data models on the posterior parameter distributions are also analyzed.

3.1 Residual characterization

Figure 3 shows residual plots for model 6C based on data models SLS and WSEP-AC. SLS is the simplest one with the assumptions of homoscedastic, independent, and Gaussian residuals, and the WSEP-AC is the most complex one without the assumptions. Model 6C is the most complex model and also the best one as ranked by Zhang et al. (2014) using Bayesian model selection. The variable a_t plotted in Figures 3a-3c and Figures 3d-3f is defined in equations (2) and (11), respectively. Figures 3a – 3c show that the three residual assumptions are violated when SLS is used because (i) the residual variance is not constant, but increases as a function of the simulated CO_2 efflux (Figure 3a); (ii) the autocorrelation function at most lags is beyond the 95% confidence

456 interval (Figure 3b); (iii) and the standard normal density function cannot adequately characterize
457 the residuals (Figure 3c). Figures 3d-f show that, after relaxing the three assumptions, the
458 processed residuals, a_t, can be well characterized by WSEP-AC. Figure 3d shows that, after
459 normalizing ε_t with the linear variance ($\sigma_t = 0.034 + 0.099 E_t$), the variation of the variance of
460 a_t becomes significantly smaller, although the variance is still not constant. Figure 3e shows that,
461 after removing a first-order autoregressive model from ε_t, a_t becomes less correlated, although the
462 correlation is not fully removed. The two coefficients of the autoregressive model are $\phi_1 = 0.989$
463 and $\phi_2 = 4.5\times10^{-6}$; the small value of ϕ_2 indicates that there is no need to attempt an autoregressive
464 model of higher order. Figure 3f shows that a_t follows the SEP distribution with the estimated
465 skewness coefficient of $\xi = 0.933$ and kurtosis coefficient of $\beta = 0.998$. As a summary, Figure
466 3 shows that it is important to examine the residuals and to determine whether a data model is
467 adequate for charactering the residuals. Although WSEP-AC still cannot perfectly characterize ε_t,
468 it is significantly better than SLS.

469 Although the Gaussian assumption used in SLS is violated for model 4C (Figure 3c), this is
470 not generally the case for other data models and soil respiration models. This is shown in Figure
471 4, which presents the quantile-quantile (Q-Q) plot for the eight data models and the three soil
472 respiration models. For SLS, WLS, SLS-AC, and WLS-AC, the theoretical quantiles are based on
473 the standard normal distribution, $N(0,1)$; for SEP, WSEP, SEP-AC, and WSEP-AC, the theoretical
474 quantiles are based on the standard skew exponential power distribution, $SEP(0,1,1,0)$. If the
475 residuals follow the assumed standard distributions, the Q-Q plots fall on the 1:1 line, which is
476 marked as the theoretical lines in Figure 4. If the residuals are Gaussian or SEP but not standard,
477 the Q-Q plots fall on a straight line but not the 1:1 line. Figures 4a and 4e show that, for all the soil
478 respiration models, the Q-Q plots of SLS and SEP deviate significantly from the theoretical lines

and exhibit fat-tail behaviors, which is an indication of outliers (Thyer et al., 2009). The deviation is reduced after accounting for autocorrelation in SLS-AC and SEP-AC, as shown in Figures 4c and 4g. It is interesting to observe from the two figures that the Q-Q plots of the three models are almost visually identical. The deviation is almost fully removed after accounting for heteroscedasticity in WLS and WSEP in that their corresponding Q-Q plots fall on the 1:1 lines, especially for models 5C and 6C, as shown in Figures 4b and 4f. However, the Q-Q plots start deviating from the 1:1 lines as shown in Figures 4d and 4h, after accounting for both heteroscedasticity and autocorrelation in WLS-AC and WSEP-AC. As a summary, Figure 4 shows that, for the numerical example of this study, either the Gaussian or the SEP distribution is valid if heteroscedasticity is accounted for in the data models. However, accounting for autocorrelation in the data models does not help improve the characterization of the residual distribution.

3.2 Posterior parameter distributions

While Figures 3 and 4 help understand validity of the three assumptions used in the data models, the impacts of the data models on estimating model parameter distributions must be evaluated separately. This section discusses the impact of the data model selection on parameter estimation with the objective of understanding if incorrect specification of the data model, will necessarily lead to biased parameter estimates. Such assessment is not a trivial task for three main reasons. First, microbial soil respiration models aggregate complex natural processes and spatial details into simpler conceptual representations. As a results several model parameters are effective values of several complex natural processes that cannot be actually measured in the field as discussed by Vrugt et al. (2013). Second, even for model parameter that can be measured in the field, since the model structure is imperfect, it can be the case that parameter values can be

accepted beyond their physically reasonable range as discussed by Pappenberger and Beven (2006). This is often undesirable, if we seek to make the models more mechanistically descriptive.

We focus our discussion on carbon use efficiency (CUE) for microbial growth since CUE is a fundamental parameter in microbial soil respiration models, and a reasonable physical range for CUE can estimated. The concept of microbial CUE(Allison et al., 2010; Bradford et al., 2008; Manzoni et al., 2012; Wieder et al., 2013) has been used to present fundamental microbial processes recent microbial enzyme models(Allison et al., 2010; German et al., 2011; Schimel and Weintraub, 2003; Wang et al., 2013). The microbial CUE, which is marked between MIC and CO2 in Figure 1, controls microbial growth, enzyme production and microbial respiration. A reasonable range of CUE can be estimated from the physical viewpoint(Tang and Riley, 2014). Sinsabaugh et al. (2013) study shows that the thermodynamic calculations support a maximum CUE of 0.60 and that methods used to estimate CUE in terrestrial systems report a mean value of 0.55. Theoretically, there no lower limit for CUE as it can approach zero, and CUE< 0.1 are reported for terrestrial ecosystems (e.g. Fernández-Martínez et al., 2014) and used in modeling studies (Li et al., 2014).

Figure 5 plots the CUE posterior marginal density of the three soil respiration models obtained using the eight data models. The physical range between zero and 0.6 is marked in yellow. Figure 5 shows that the CUE posterior parameter distribution for Model 6C for all likelihood functions that does not account for autocorrelation are within a reasonable physical range. For models 4C and 5C, the posterior parameter samples are outside the physical range for six data models. For model 4C, the posterior parameters are within the physical range only for data models SEP and WSEP; for model 5C, the two data models are WLS and WSEP. It is not surprising to find the posterior parameter distribution of models 4C and 5C, which have a certain degree of model

structure error, to be out of the plausible physical range. This can be attributed to two reasons. First, the model solution can be biased toward the missing processes in the model structure such as the additional carbon pool in both 4C and 5C or the explicit accounting for soil moister in 4C. Second, biased parameter estimation can compensate for model structure inadequacy and other sources of discrepancy in both the physical model and the statistical model.

In addition, it is important to understand how accounting for autocorrelation, heteroscedasticity and non-Gaussian residuals can affect the parameter estimation. First, we obtained biased parameter estimates that is out the reasonable physical range when autocorrelation is explicitly accounted for as shown in Figure 5e-h. This may suggest again that accounting for heteroscedasticity is desirable but accounting for autocorrelation is not. A possible reason is that filtering autocorrelation may reduce the residual space such that the transformed residual space cannot correspond to the parameter space of the models. In other words, parameter information may be lost due to filtering out autocorrelation. However, it is not fully understood why this does not occur for the model 6C under data model SLS-AC, and more research is warranted. Second, unlike accounting for auto-correlation, accounting only for heteroscedasticity (i.e. WLS and WSEP) since this will only amplify or reduce the variance without affecting the structure of the residual space. Figure 5c-d shows that account for heteroscedasticity (i.e. WLS and WSEP) tends to improve the parameter estimation in comparison with homoscedastic data models (i.e. SLS and SEP) shown in Figure 5a-b. Finally, with respect to non-Gaussian residuals, Schoups and Vrugt (2010) proposes that the peaked pdf of the SEP with heavier tails compared to Gaussian pdf is useful for making parameter inference robust against outliers. To a certain degree, this can be substantiated by the results in Figure 5a-d, such that SEP and WSEP provide more favorable parameter estimates than SLS and WLS.

Finally, from Figure 5 we can also notice that the posterior parameter distribution of SLS (Figure 5a) is very narrow. This narrow posterior parameter distribution of SLS compared to other likelihood functions can be attributed to several reasons. Since SEP can have heavier tails than Gaussian distribution, this can further increase the samples acceptance ratio from tails resulting in wider distribution (Figure 5b). In addition, accounting for heteroscedasticity will wider the posterior parameter distribution (Figure 5c) due to accepting higher variances at peak effluxes. Moreover, filtering correlation (Figure 5e-h) increases the entropy.

4. Results of Predictive Performance

Based on the last one third of the CO_2 efflux observations, a cross-validation test was conducted for all the 24 models, the combinations of three soil respiration models and eight data models. Given the cross-validation period, the predictive performance is examined using the four statistical metrics that are defined in Section 2.5. The metrics are also calculated for the calibration period. This is not to perform Bayesian model selection given the calibration data, but to better understand the impact of data models. For each calibration and each cross-validation data, a prediction ensemble is generated from the two perspectives of parametric uncertainty only and total uncertainty, as presented in Section 4.1 and 4.2, respectively.

4.1 Predictive performance with parametric uncertainty of soil respiration model

In this section the ensemble is generated by running the soil respiration models with the posterior samples (obtained from the Bayesian inference) of the physical model parameters. In other words, the ensemble addresses parametric uncertainty of the soil respiration models only. Considering the relative contribution of parametric uncertainty only will provide insights for modeling approaches that attempt to segregate various sources of uncertainty (e.g. Thyer et al., 2009 ; Tsai and Elshall, 2013).

570 The four statistics above (i.e. NSME, sharpness, coverage, and RMS) are calculated for the
571 three soil respiration models and the eight data models. Taking data models SLS and WSEP-AC
572 as an example, Figure 6 plots the data (for the calibration and cross-validation periods separately)
573 along with the mean and 95% credible intervals of the prediction ensemble for the three models.
574 Figure 6 shows that the data models affect model simulations for all the models. The statistics,
575 especially RMS, indicate that WSEP-AC has better predictive performance than SLS. This is most
576 visually obvious for model 6C during the cross-validation period after 330 days, as the prediction
577 ensemble of SLS (Figure 6k) cannot cover the observations, unlike the prediction ensemble of
578 WSEP-AC can (Figure 6l). This conclusion that WSEP-AC outperforms SLS agrees with that
579 drawn from Figures 3 and 4.
580 Figure 7 plots the four statistics for all the soil respiration models and data models. Figures 7a
581 and 7b show the predictive performance with respect to the central mean tendency using NSME
582 for both the calibration and cross-validation periods respectively. The results indicate that the low
583 fidelity model 4C under all data models will over-fit the data resulting in biased predictions such
584 that the NSME values become significantly worse (from 0.6 to -0.6) from the calibration to the
585 cross-validation period. This is confirmed by the visual inspection of Figures 6a, 6b, 6g, and 6h
586 for data models SLS and WSEP-AC. For models 5C and 6C, their NSME values vary with the
587 data models; and the central mean accuracy is the worst for SLS-AC that considers only
588 autocorrelation.
589 With respect to parametric uncertainty estimation, Figures 7c and 7d show sharpness generally
590 increases when the three assumptions in the data models are gradually relaxed from SLS to WSEP-
591 AC. This is even more obvious during the validation period. Given that the prediction ensemble
592 does not center on the data, the increasing sharpness is desirable as it improves reliability. This is

593 confirmed by the reliability plots in Figures 7e and 7f. The exceptions are again SLS-AC and SEP-
594 AC that generally have the lowest coverage.

595 With respect to the overall predictive performance, the same variation pattern and exception
596 are also observed in the RMS plots in Figures 7g and 7h. This is not surprising because RMS is
597 the metric that can be used to measure all the three criteria (central mean tendency, sharpness, and
598 reliability). Since the prediction ensemble is not centered on the data, the sharpness and reliability
599 are the decisive factors for evaluating the predictive performance.

600 As a summary, while it is necessary to account for heteroscedasticity in a data model, caution
601 is needed when accounting for autocorrelation in the manner described in Section 2.1. In addition,
602 after comparing the RMS values of the residuals using the Gaussian and SEP distributions, the
603 conclusion is that the SEP distribution outperforms the Gaussian distribution with respect to
604 predictive performance. Finally, uncertainty underestimation as evident by the very small
605 predictive coverage. The underestimation of uncertainty for all the physical models with all
606 likelihood functions makes sense because only parametric uncertainty is considered. Considering
607 the overall predictive uncertainty is the subject of the next section.

608 **4.2 Predictive performance with total uncertainty**

609 The simulated output $\mathbf{Y}(\theta_p)$ will generally not be equal to the observed output $\mathbf{d}$ and we have
610 a residual term $\mathbf{e}$ due to measurement, input and model structure errors such that $\mathbf{d} = \mathbf{Y}(\theta_p) + \mathbf{e}$.
611 Accounting for the error term $\mathbf{e}$ can be through separating various error terms. For example, in
612 section 4.1 we obtained uncertainty due to the physical model parameters. Accounting for other
613 sources of uncertainty can be done using a single model approach (e.g. Thyer et al., 2009) or a
614 multi-model approach (e.g. Tsai and Elshall, 2013). Alternatively, we can quantify the uncertainty
615 based on total residuals that separates out parametric uncertainty, so the residual error includes

616 measurement, model input, and model structure uncertainty (e.g. Thyer et al., 2009; Schoups and
617 Vrugt, 2010). This lumped approach is based on sampling the residuals model $\mathbf{e}(\theta_e)$ with
618 parameters θ_e. SLS has one fixed parameter that is the constant variance and other data models
619 have two to six parameters. Thus in this section the prediction ensemble addresses parametric
620 uncertainty of not only the soil respiration models but also the data models. When generating the
621 prediction ensemble in the procedure described by Schoups and Vrugt (2010), an ensemble of
622 residuals is first generated by running the data models with posterior samples of the data model
623 parameters for the positive carbon efflux domain; the residual ensemble is then added to the
624 prediction ensemble generated in Section 4.1.

625 We start by the visual assessment of the predictive performance. Figure 8 is similar to Figure
626 6 with the exception that Figure 8 considers the overall all predictive uncertainty (i.e. parametric
627 and output uncertainty), while Figure 6 considers the parametric uncertainty only. Figure 8 reveals
628 a practical observation about accounting for the overall uncertainty through the lumped approach
629 of sampling the residuals model. Figure 8b shows that despite the wide prediction interval of model
630 4C, which has significant model structure error, it could not capture the birch pulse around day
631 180. This clearly indicates that proper modeling of the residuals will not make-up for of significant
632 model structure error.

633 Figure 9 plots the four statistics (NSME, sharpness, predictive coverage, and RMS) of the three
634 models under the eight data models to assess the predictive performance. First with respect to
635 central mean tendency, The NSME values in Figures 9a-9b are visually the same as those in
636 Figures 7a-7b, indicating that the central mean accuracy under parametric uncertainty is the same
637 as that under predictive uncertainty.

With respect to uncertainty, the values of sharpness and predictive coverage increase substantially (Figures 9c – 9f). In particular, Figures 9e and 9f show that, except for SLS and SEP, the predictive coverage of the rest of the six data models are close to 100% for all the three soil respiration models, indicating that the prediction intervals cover almost all the data. This is demonstrated in Figures 6 for WSEP-AC. Similar to Figures 7c and 7d, Figures 9c and 9d also show a general pattern that the sharpness increases when the three assumptions in the data models are gradually relaxed from SLS to WSEP-AC. The data models that account for autocorrelation are still the exceptions.

With respect to the overall predictive performance, the RMS values are largely determined by mean accuracy and sharpness as the predictive coverage is similar for different data models. Figures 9g and 9h of RMS show that the predictive performance of the four data models that account for autocorrelation is worse than that of the other four data models. This suggests again that one needs to be cautious when building autocorrelation into a data model. This is consistent with the finding of Evin et al. (2013, 2014) that accounting for autocorrelation before accounting for heteroscedasticity or jointly accounting for autocorrelation and heteroscedasticity can result in poor predictive performance. In summary, Figures 9g and 9h show for both the calibration and prediction periods that accounting for heteroscedasticity (i.e. WLS and WSEP) will give the best overall predictive performance, and accounting for autocorrelation without heteroscedasticity (i.e. SLS-AC and SEP-AC) will give the worst overall predictive performance. Finally, for the three soil respiration models, RMS shows that model 4C has the worst predictive performance for both the calibration and cross-validation data. Generally speaking, the high fidelity model 6C outperforms model 5C for both the calibration and cross-validation data, which justifies the complexity of model 6C.

661 To demonstrate the impacts of the data models on predictive performance of the soil respiration
662 models, Figure 10 plots the model simulations and predictions given by model 6C during the
663 calibration and cross-validation periods using all the eight data models.

664 In Figure 10 we try to understand the predictive performance characteristics of the different
665 data models by looking at the predictive performance of model 6C. Specific predictive
666 performance patterns can be identified. Figures 10-a-d show that SLS and SEP have similar
667 predictive performance with SEP generally having better predictive performance especially during
668 the validation period. Accounting for heteroscedasticity using WLS as shown in Figures 10e and
669 10h will make the predictions more sensitive to peck carbon effluxes and will generally improve
670 the predictive coverage on the expense of sharpness and the central mean tendency. WLS and
671 WSEP have similar predictive performance. However, WSEP maintains slightly better central
672 mean tendency and overall predictive performance than WLS. Accounting for autocorrelation
673 using SLS-AC and SEP-AC as shown in Figures 10i and 10l reduces the information content of
674 the residuals, and thus resulting in wider uncertainty bands and insensitivity to peak carbon
675 effluxes as compared to SLS and SEP (Figures 10a-d). This resulted in deteriorating the sharpness,
676 the central mean tendency and the capturing of peak carbon fluxes, especially during the validation
677 period. Accounting for both heteroscedasticity and autocorrelation using WLS-AC and WSEP-
678 AC will make the inference robust against peck carbon effluxes, yet due to the loss of information
679 content uncertainty bands are still wider and uncertainty becomes overestimated especially during
680 validation period as compared to WLS and WSEP. The results of Models 4C and 5C, which are
681 not shown here, also show the same prediction patterns with respect to non-Gaussian residuals,
682 heteroscedasticity and autocorrelation.

From figure 10 we also notice that data models that have good overall predictive performance as measured by RMS during the calibration period will maintain this good predictive performance during the validation period. For model 6C, RMS values for the calibration and validation periods are very well correlated with a correlation coefficient of 0.92. However, we note that for models 4C and 5C the overall predictive performance during the calibration and validation periods are not that well correlated as 6C, with correlation coefficients of 0.52 for model 4C and 0.61 for model 5C. This suggests that model 6C is more robust than 4C and 5C for forecasting and hindcasting.

5. Conclusions

In parameter estimation and prediction of soil carbon fluxes to the atmosphere we often assume that residuals, which include observation, model input, model errors, are normally distributed, homoscedastic and uncorrelated. We studied these assumptions by calibrating three microbial enzyme models, which have varying degrees of model structure errors. We tested eight data models starting with the standard least squares (SLS) and skew exponential power (SEP) data models that assume homoscedastic and non-correlated residuals. Given these two distributions, we evaluated six other data models that account for heteroscedasticity (WLS and WSEP), autocorrelation (SLS-AC and SEP-AC) and joint inversion of heteroscedasticity and autocorrelation (WLS-AC and WSEP-AC). To our knowledge this is the first study that provide such detailed analysis soil reparation inverse modeling. We also used three solid respiration models with different degrees of model fidelity (i.e. model realism) and model complexity (i.e. number of model parameters), to understand the impact of model discrepancy on the calibration results under different data models. We analyzed the calibration results with respect to (i) residual characterization, (ii) parameter estimation, (iii) predictive performance and (iv) impact of model discrepancy. The main findings of this study can be summarized as follows:

(i) With respect to residual characterization, residual analysis results suggest that the common assumption of not accounting for heteroscedasticity and autocorrelation of residuals (i.e. SLS and SEP) results in poor characterization of residuals. Explicit accounting for heteroscedasticity (i.e. WLS and WSEP) can result in good characterization of the residuals, and is followed by joint the inversion of heteroscedasticity and autocorrelation (i.e. WSL-AC and WSEP-AC). Accounting for autocorrelation only (i.e. SLS-AC and SEP-AC) may not improve much the characterization of the residuals.

(ii) With respect to parameter estimation, we focused on carbon use efficiency (CUE), which is a central parameter in soil respiration modeling. We found the SLS with relatively reasonable posterior parameter distribution for CUE, yet very narrow posterior. Data models consider autocorrelation (i.e. SLS-AC, SEP-AC, WLS-AC and WSEP-AC) tend to generally yield CUE estimates that are physically non-reasonable. We speculate that filtering correlation can affect the mapping of the model physics (as implicitly included in the residuals) into the likelihood space, which might result in biased parameter estimates that are physically unreasonable.

(iii) With respect to predictive performance, we assessed the central mean tendency, uncertainty bands and the overall predictive performance for both the calibration and the cross-validation periods. Results show that accounting for autocorrelation (i.e. SLS-AC, SEP-AC, WLS-AC, and WSEP-AC) deteriorates the predicative performance, such that the predictive performance is inferior to SLS in terms of the central mean tendency and overall predictive performance, especially during the cross-validation period. Results also indicates that using a SEP distribution can potentially improve the predictive performance. The same is true for accounting for heteroscedasticity. Using SEP distribution and accounting for heteroscedasticity (i.e. WSEP) can potentially improve the predictive performance.

729 (iv) With respect to the impact of model discrepancy, the high fidelity complex model (6C)
730 gives the best results with respect to parameter estimation and predictive performance. Model 6C
731 generally maintained its superior performance under different data models. This justifies the
732 complexity of model 6C relative to model 5C that has one less carbon pool. Model 4C that has a
733 low fidelity model with only four carbon pools and lacks the explicit representation of soil moisture
734 control, maintains its poor performance for different data models.

735 From the empirical findings of this research we conclude the following: (i) Not accounting for
736 heteroscedasticity and autocorrelation using a Gaussian or non-Gaussian data model might not
737 necessarily result in biased parameter estimates or biased predictions with respect to central mean
738 tendency, but will definitely underestimate uncertainty resulting in lower overall predictive
739 performance. (ii) Using a non-Gaussian residual error model can improve the parameter estimates,
740 and the predictive performance with respect to central mean tendency and uncertainty estimation.
741 (iii) Accounting for heteroscedasticity will definitely improve the uncertainty estimation with
742 respect to reliability at the cost of having a wider predictive interval. (iv) This study confirms the
743 empirical findings and theoretical analysis (Evin et al., 2013; 2014; Ammann et al. 2018) that
744 separate accounting for autocorrelation or joint inversion of correlation and heteroscedasticity can
745 be problematic. By drawing on similarity from surface hydrology, the study of Ammann et al.
746 (2018) suggests that this might be attributed to non-stationarity due to wet-dry periods with half-
747 hourly data. Accounting for non-stationarity (Smith et al., 2010b, Ammann et al. 2018) could
748 address this problem. Relatively poor performance with respect to autocorrelation can be also
749 attributed to the implementation scheme. The inference scheme such as joint inference as in this
750 study, post-processing inference approach for autocorrelation (Evin et al., 2013; 2014), residuals
751 transformation approach (e.g. Lu et al., 2013) or other strategies (Li et al., 2015, 2016a) could have

752 an impact. Yet Ammann et al., (2018) study states that the joint inversion is still preferred, and
753 understanding the conditions where accounting for auto-correlation can be achieved remain poorly
754 understood. Further investigation of this point is warranted in a future study.

755 The above conclusions are subject to several limitations. First, the conclusions are specific to
756 the soil respiration models developed and validated for semi-arid savannah. Performance
757 variations across different soil respiration models with different levels of complexities is possible.
758 Second, the conclusions are conditioned on the data that were obtained at the half-hour interval
759 over a one-year period. Different conclusions are possible if the data are thinned to daily or weekly
760 scales or data of longer observation periods are used. Third, the study investigates effects of the
761 residual assumptions of formal likelihood functions through direct conditioning of the residuals
762 model parameters, yet this can also be done through other approaches such as residuals
763 transformation (Thiemann et al., 2001), autorgressive bias model (Del Giudice et al., 2013),
764 approximate Bayesian computation (Sadegh and Vrugt, 2013), data assimliation (Spaaks and
765 Bouten, 2013). Comparing different methods for accounting the residual assumptions are beyond
766 the scope of this work. Fourth, this study focuses on formal Bayesian computation using formal
767 likelihood functions, and comparison with other inference functions such as informal likelihood
768 functions or approximate Bayesian computation is warranted in a future study.

769 Based on the aforesaid conclusions and limitations, we recommend to start calibrating soil
770 respiration models with simple SLS or SEP likelihood function. If the residuals characterization is
771 adequate (e.g. Scharnagl et al., 2011), then the underlying assumptions are met. Otherwise,
772 increase complexity of the data model until satisfactory results are obtained in terms of residuals
773 characterization, posterior parameter estimation and predictive performance. Although the
774 empirical findings of this study provide general guidelines for data model selection of microbial

soil respiration models, more comparative studies are needed to validate and refute the findings of this study.

Acronyms

4C	Four carbon pool model
5C	Five carbon pool model
6C	Six carbon pool model
CUE	Microbial carbon use efficiency
DOC	Dissolved organic carbon
ENZ	Enzymes
MCMC	Markov chain Monte Carlo
MIC	Microbial biomass
NSME	Nash-Sutcliffe model efficiency
PDF	Probability density function
RMS	Relative model score
SEP	Skew exponential power distribution
SEP-AC	Skew exponential power distribution with autocorrelation
SLS	Standard least square
SLS-AC	Standard least square with autocorrelation
SOC	Soil organic carbon
WLS	Weighted least squared
WLS-AC	Weight least square with autocorrelation
WSEP	Weighted skew exponential power distribution
WSEP-AC	Weighted skew exponential power distribution with autocorrelation

Code and data availability

The data and codes and models used to produce this paper are available on contact of the corresponding author at mye@fsu.edu. We cannot publicly share the workflow because MT-DREAM$_{(ZS)}$ code (Laloy and Vrugt, 2012) , which is a main component in the workflow, is in the process of becoming a commercial code.

Author contributions

ASE developed and implemented the code for the eight data models for soil respiration modeling, and prepared the manuscript with contribution of all co-authors. MY developed the research idea and outline, and supervised the research implementation. GN developed the soil respiration models. GAB collected and processed the eddy-covariance data used for model calibration.

Competing interests

The authors declare that they have no conflict of interest.

Acknowledgement

This work was supported by the Department of Energy Early Career Award, DE-SC0008272 and U.S. National Science Foundation Award# OIA-1557349.

References

Ahrens, B., Reichstein, M., Borken, W., Muhr, J., Trumbore, S. E. and Wutzler, T.: Bayesian calibration of a soil organic carbon model using ΔC measurements of soil organic carbon and heterotrophic respiration as joint constraints, Biogeosciences, 11(8), 2147–2168, doi:10.5194/bg-11-2147-2014, 2014.

Allison, S. D., Wallenstein, M. D. and Bradford, M. A.: Soil-carbon response to warming dependent on microbial physiology, Nat. Geosci., 3, 336 [online] Available from: http://dx.doi.org/10.1038/ngeo846, 2010.

Ammann, L., Reichert, P. and Fenicia, F.: A framework for likelihood functions of deterministic hydrological models, Hydrol. Earth Syst. Sci., (August), 2018.

Bagnara, M., Sottocornola, M., Cescatti, A., Minerbi, S., Montagnani, L., Gianelle, D. and Magnani, F.: Bayesian optimization of a light use ef fi ciency model for the estimation of daily gross primary productivity in a range of Italian forest ecosystems, Ecol. Modell., 306, 57–66, doi:10.1016/j.ecolmodel.2014.09.021, 2015.

Bagnara, M., Oijen, M. Van, Cameron, D., Gianelle, D., Magnani, F. and Sottocornola, M.: Bayesian calibration of simple forest models with multiplicative mathematical structure : A case study with two Light Use E ffi ciency models in an alpine forest, Ecol. Modell., 371(January), 90–100, doi:10.1016/j.ecolmodel.2018.01.014, 2018.

832 Barr, J. G., Engel, V., Fuentes, J. D., Fuller, D. O. and Kwon, H.: Modeling light use efficiency in
833 a subtropical mangrove forest equipped with CO2eddy covariance, Biogeosciences, 10(3),
834 2145–2158, doi:10.5194/bg-10-2145-2013, 2013.
835 Barron-gafford, G. A., Cable, J. M., Bentley, L. P., Scott, R. L., Huxman, T. E., Jenerette, G. D.
836 and Ogle, K.: Quantifying the timescales over which exogenous and endogenous conditions
837 affect soil respiration, New Phytol., 2014.
838 Barron-Gafford, G. A., Scott, R. L., Jenerette, G. D. and Huxman, T. E.: The relative controls of
839 temperature, soil moisture, and plant functional group on soil CO2 efflux at diel, seasonal,
840 and annual scales, J. Geophys. Res. Biogeosciences, 116(1), 1–16,
841 doi:10.1029/2010JG001442, 2011.
842 Berryman, E. M., Frank, J. M., Massman, W. J. and Ryan, M. G.: Agricultural and Forest
843 Meteorology Using a Bayesian framework to account for advection in seven years of
844 snowpack CO 2 fl uxes in a mortality-impacted subalpine forest, Agric. For. Meteorol.,
845 249(April 2017), 420–433, doi:10.1016/j.agrformet.2017.11.004, 2018.
846 Box, E. P. and Tiao, G. C. (1992), Bayesian Inference in Statistical Analysis, 588 pp., Wiley, New
847 York.
848 Braakhekke, M. C., Beer, C., Schrumpf, M., Ekici, A., Ahrens, B., Hoosbeek, M. R., Kruijt, B.,
849 Kabat, P. and Reichstein, M.: The use of radiocarbon to constrain current and future soil
850 organic matter turnover and transport in a temperate forest, J. Geophys. Res. Biogeosciences,
851 372–391, doi:10.1002/2013JG002420.Received, 2014.
852 Bradford, M. A., Davies, C. A., Frey, S. D., Maddox, T. R., Melillo, J. M., Mohan, J. E., Reynolds,
853 J. F., Treseder, K. K. and Wallenstein, M. D.: Thermal adaptation of soil microbial
854 respiration to elevated temperature, Ecol. Lett., 11(12), 1316–1327, doi:10.1111/j.1461-

855 0248.2008.01251.x, 2008.
856 Braswell, B. H., Sacks, W. J., Linder, E. and Schimel, D. S.: Estimating diurnal to annual
857 ecosystem parameters by synthesis of a carbon flux model with eddy covariance net
858 ecosystem exchange observations, Glob. Chang. Biol., 335–355, doi:10.1111/j.1365-
859 2486.2005.00897.x, 2015.
860 Cable, J. M., Ogle, K., Williams, D. G., Weltzin, J. F. and Huxman, T. E.: Soil Texture Drives
861 Responses of Soil Respiration to Precipitation Pulses in the Sonoran Desert : Implications
862 for Climate Change, Ecosystems, 961–979, doi:10.1007/s10021-008-9172-x, 2008.
863 Cable, J. M., Ogle, K., Lucas, R. W., Huxman, T. E., Loik, M. E., Smith, S. D., Tissue, D. T.,
864 Ewers, B. E., Pendall, E., Welker, J. M., Charlet, T. N., Cleary, M., Griffith, A., Nowak, R.
865 S., Rogers, M., Steltzer, H., Sullivan, P. F. and Gestel, N. C. Van: The temperature responses
866 of soil respiration in deserts : a seven desert synthesis, Biogeochemistry, 71–90,
867 doi:10.1007/s10533-010-9448-z, 2011.
868 Chevallier, F. and O'Dell, C. W.: Error statistics of Bayesian CO2flux inversion schemes as seen
869 from GOSAT, Geophys. Res. Lett., 40(6), 1252–1256, doi:10.1002/grl.50228, 2013.
870 Correia, A. C., Minunno, F., Caldeira, M. C., Banza, J., Mateus, J., Carneiro, M., Wingate, L.,
871 Shvaleva, A., Ramos, A., Jongen, M., Bugalho, M. N., Nogueira, C., Lecomte, X. and
872 Pereira, J. S.: Agriculture , Ecosystems and Environment Soil water availability strongly
873 modulates soil CO 2 efflux in different Mediterranean ecosystems : Model calibration using
874 the Bayesian approach, Agric. Ecosyst. Environ., 161, 88–100,
875 doi:10.1016/j.agee.2012.07.025, 2012.
876 Davidson, E. A. and Janssens, I. A.: Temperature sensitivity of soil carbon decomposition and
877 feedbacks to climate change, Nature, 440, 165 [online] Available from:

878 http://dx.doi.org/10.1038/nature04514, 2006.
879 Davidson, E. A., Samanta, S., Caramori, S. S. and Savage, K.: The Dual Arrhenius and Michaelis–
880 Menten kinetics model for decomposition of soil organic matter at hourly to seasonal time
881 scales, Glob. Chang. Biol., 18(1), 371–384, doi:10.1111/j.1365-2486.2011.02546.x, 2011.
882 Du, Z., Nie, Y., He, Y., Yu, G. and Wang, H.: Tellus B : Chemical and Physical Meteorology
883 Complementarity of flux- and biometric-based data to constrain parameters in a terrestrial
884 carbon model Complementarity of flux- and biometric-based data to constrain parameters in
885 a terrestrial carbon model, Tellus B Chem. Phys. Meteorol., 0889,
886 doi:10.3402/tellusb.v67.24102, 2015.
887 Du, Z., Zhou, X., Shao, J., Yu, G., Wang, H., Zhai, D., Xai, J. and Luo, Y.: Journal of Advances
888 in Modeling Earth Systems, J. Adv. Model. Earth Syst., 548–565,
889 doi:10.1002/2016MS000687.Received, 2017.
890 Elshall, A. S. and Tsai, F. T.-C.: Constructive epistemic modeling of groundwater flow with
891 geological structure and boundary condition uncertainty under the Bayesian paradigm, J.
892 Hydrol., 517, doi:10.1016/j.jhydrol.2014.05.027, 2014.
893 Elshall, A. S., Ye, M., Pei, Y., Zhang, F., Niu, G.-Y. and Barron-Gafford, G. A.: Relative model
894 score: a scoring rule for evaluating ensemble simulations with application to microbial soil
895 respiration modeling, Stoch. Environ. Res. Risk Assess., doi:10.1007/s00477-018-1592-3,
896 2018a.
897 Elshall, A. S., Ye, M., Pei, Y., Zhang, F., Niu, G.-Y. and Barron-Gafford, G. A.: Relative model
898 score: a scoring rule for evaluating ensemble simulations with application to microbial soil
899 respiration modeling, Stoch. Environ. Res. Risk Assess., 32(10), 2809–2819,
900 doi:10.1007/s00477-018-1592-3, 2018b.

Evin, G., Kavetski, D., Thyer, M. and Kuczera, G.: Pitfalls and improvements in the joint inference of heteroscedasticity and autocorrelation in hydrological model calibration, Water Resour. Res., 49(7), 4518–4524, doi:10.1002/wrcr.20284, 2013.

Evin, G., Thyer, M., Kavetski, D., McInerney, D. and Kuczera, G.: Comparison of joint versus postprocessor approaches for hydrological uncertainty estimation accounting for error autocorrelation and heteroscedasticity, Water Resour. Res., 50(3), 2350–2375, doi:10.1002/2013WR014185, 2014.

Fernández-Martínez, M., Vicca, S., Janssens, I. A., Sardans, J., Luyssaert, S., Campioli, M., Chapin III, F. S., Ciais, P., Malhi, Y., Obersteiner, M., Papale, D., Piao, S. L., Reichstein, M., Rodà, F. and Peñuelas, J.: Nutrient availability as the key regulator of global forest carbon balance, Nat. Clim. Chang., 4, 471 [online] Available from: http://dx.doi.org/10.1038/nclimate2177, 2014.

Gelman, A. and Rubin, D. B.: Inference from Iterative Simulation Using Multiple Sequences, Stat. Sci., 7(4), 457–472, doi:10.1214/ss/1177011136, 1992.

German, D. P., Marcelo, K. R. B., Stone, M. M. and Allison, S. D.: The Michaelis–Menten kinetics of soil extracellular enzymes in response to temperature: a cross-latitudinal study, Glob. Chang. Biol., 18(4), 1468–1479, doi:10.1111/j.1365-2486.2011.02615.x, 2011.

Del Giudice, D., Honti, M., Scheidegger, A., Albert, C., Reichert, P. and Rieckermann, J.: Improving uncertainty estimation in urban hydrological modeling by statistically describing bias, Hydrol. Earth Syst. Sci., 17(10), 4209–4225, doi:10.5194/hess-17-4209-2013, 2013.

Gragne, A. S., Sharma, A., Mehrotra, R. and Alfredsen, K.: Improving real-time inflow forecasting into hydropower reservoirs through a complementary modelling framework, Hydrol. Earth Syst. Sci., 19(8), 3695–3714, doi:10.5194/hess-19-3695-2015, 2015.

924 Hararuk, O., Xia, J. and Luo, Y.: Evaluation and improvement of a global land model against soil
925 carbon data using a Bayesian Markov chain Monte Carlo method, J. Geophys. Res.
926 Biogeosciences, 119(3), 403–417, doi:10.1002/2013JG002535, 2014.
927 Hashimoto, S., Morishita, T., Sakata, T., Ishizuka, S., Kaneko, S. and Takahashi, M.: Simple
928 models for soil CO2, CH4, and N2O fluxes calibrated using a Bayesian approach and multi-
929 site data, Ecol. Modell., 222(7), 1283–1292, doi:10.1016/j.ecolmodel.2011.01.013, 2011.
930 He, H., Meyer, A., Jansson, P., Svensson, M., Rütting, T. and Klemedtsson, L.: Simulating
931 ectomycorrhiza in boreal forests : implementing ectomycorrhizal fungi model MYCOFON
932 in CoupModel (v5), Geosci. Model Dev., 725–751, 2018.
933 Hilton, T. W., Davis, K. J. and Keller, K.: Evaluating terrestrial CO2flux diagnoses and
934 uncertainties from a simple land surface model and its residuals, Biogeosciences, 11(2), 217–
935 235, doi:10.5194/bg-11-217-2014, 2014.
936 Hoeting, J. A., Madigan, D., Raftery, A. E. and Volinsky, C. T.: Bayesian model averaging: a
937 tutorial (with comments by M. Clyde, David Draper and E. I. George, and a rejoinder by the
938 authors, Stat. Sci., 14(4), 382–417, doi:10.1214/ss/1009212519, 1999.
939 Högberg, P. and Read, D. J.: Towards a more plant physiological perspective on soil ecology,
940 Trends Ecol. Evol., 21(10), 548–554, doi:10.1016/j.tree.2006.06.004, 2006.
941 Hublart, P., Ruelland, D., De Cortázar-Atauri, I. G., Gascoin, S., Lhermitte, S. and Ibacache, A.:
942 Reliability of lumped hydrological modeling in a semi-arid mountainous catchment facing
943 water-use changes, Hydrol. Earth Syst. Sci., 20(9), 3691–3717, doi:10.5194/hess-20-3691-
944 2016, 2016.
945 Ishikura, K., Yamada, H., Toma, Y., Takakai, F., Darung, U., Limin, A. and Limin, S. H.: Soil
946 Science and Plant Nutrition Effect of groundwater level fluctuation on soil respiration rate

947 of tropical peatland in Central Kalimantan , Indonesia, Soil Sci. Plant Nutr., 63(1), 1–13,
948 doi:10.1080/00380768.2016.1244652, 2017.
949 Janssens, I. A., Freibauer, A., Ciais, P., Smith, P., Nabuurs, G.-J., Folberth, G., Schlamadinger, B.,
950 Hutjes, R. W. A., Ceulemans, R., Schulze, E.-D., Valentini, R. and Dolman, A. J.: Europe's
951 terrestrial biosphere absorbs 7 to 12% of European anthropogenic CO2 emissions., Science,
952 300(5625), 1538–42, doi:10.1126/science.1083592, 2003.
953 Katz, R. W., Craigmile, P. F., Guttorp, P., Haran, M., Sansó, B. and Stein, M. L.: Uncertainty
954 analysis in climate change assessments, Nat. Clim. Chang., 3, 769 [online] Available from:
955 http://dx.doi.org/10.1038/nclimate1980, 2013.
956 Kavetski, D., Franks, S. W. and Kuczera, G.: Confronting Input Uncertainty in Environmental
957 Modelling, Calibration Watershed Model., doi:doi:10.1029/WS006p0049, 2013.
958 Keenan, T. F., Davidson, E., Moffat, A. M., Munger, W. and Richardson, A. D.: Using model-data
959 fusion to interpret past trends, and quantify uncertainties in future projections, of terrestrial
960 ecosystem carbon cycling, Glob. Chang. Biol., 18(8), 2555–2569, doi:10.1111/j.1365-
961 2486.2012.02684.x, 2012.
962 Kim, Y., Nishina, K., Chae, N., Park, S. J., Yoon, Y. J. and Lee, B. Y.: Constraint of soil moisture
963 on CO 2 efflux from tundra lichen , moss , and tussock in Council , Alaska , using a
964 hierarchical Bayesian model, Biogeosciences, 5567–5579, doi:10.5194/bg-11-5567-2014,
965 2014.
966 Klemedtsson, L., Jansson, P. E., Gustafsson, D., Karlberg, L., Weslien, P., Von Arnold, K.,
967 Ernfors, M., Langvall, O. and Lindroth, A.: Bayesian calibration method used to elucidate
968 carbon turnover in forest on drained organic soil, Biogeochemistry, 89(1), 61–79,
969 doi:10.1007/s10533-007-9169-0, 2008.

970 Laloy, E. and Vrugt, J. A.: High-dimensional posterior exploration of hydrologic models using
971 multiple-try DREAM(ZS) and high-performance computing, Water Resour. Res., 48(1),
972 doi:10.1029/2011WR010608, 2012.
973 Li, J., Wang, G., Allison, S. D., Mayes, M. A. and Luo, Y.: Soil carbon sensitivity to temperature
974 and carbon use efficiency compared across microbial-ecosystem models of varying
975 complexity, Biogeochemistry, 119, 67–84 [online] Available from:
976 http://www.jstor.org/stable/24716883, 2014.
977 Li, M., Wang, Q. J., Bennett, J. C. and Robertson, D. E.: A strategy to overcome adverse effects
978 of autoregressive updating of streamflow forecasts, Hydrol. Earth Syst. Sci., 19(1), 1–15,
979 doi:10.5194/hess-19-1-2015, 2015.
980 Li, M., Wang, Q. J., Bennett, J. C. and Robertson, D. E.: Error reduction and representation in
981 stages (ERRIS) in hydrological modelling for ensemble streamflow forecasting, Hydrol.
982 Earth Syst. Sci., 20(9), 3561–3579, doi:10.5194/hess-20-3561-2016, 2016a.
983 Li, Q., Xia, J., Shi, Z., Huang, K., Du, Z. and Lin, G.: Variation of parameters in a Flux-Based
984 Ecosystem Model across 12 sites of terrestrial ecosystems in the conterminous USA, Ecol.
985 Modell., 336, 57–69, doi:10.1016/j.ecolmodel.2016.05.016, 2016b.
986 Lu, D., Ye, M., Meyer, P. D., Curtis, G. P., Shi, X., Niu, X.-F. and Yabusaki, S. B.: Effects of error
987 covariance structure on estimation of model averaging weights and predictive performance,
988 Water Resour. Res., 49(9), 6029–6047, doi:10.1002/wrcr.20441, 2013.
989 Luo, Y., Ogle, K., Tucker, C., Fei, S., Gao, C., LaDeau, S., Clark, J. S. and Schimel, D. S.:
990 Ecological forecasting and data assimilation in a data-rich era, Ecol. Appl., 21(5), 1429–
991 1442, doi:10.1890/09-1275.1, 2011.
992 Luo, Y., Keenan, T. F. and Smith, M.: Predictability of the terrestrial carbon cycle, Glob. Chang.

993 Biol., 21(5), 1737–1751, doi:10.1111/gcb.12766, 2014.
994 Manzoni, S., Taylor, P., Richter, A., Porporato, A. and Ågren, G. I.: Environmental and
995 stoichiometric controls on microbial carbon-use efficiency in soils, New Phytol., 196(1), 79–
996 91, doi:10.1111/j.1469-8137.2012.04225.x, 2012.
997 McInerney, D., Thyer, M., Kavetski, D., Lerat, J. and Kuczera, G.: Improving probabilistic
998 prediction of daily streamflow by identifying Pareto optimal approaches for modeling
999 heteroscedastic residual errors, Water Resour. Res., 53, 2199–2239,
1000 doi:10.1002/2016WR019168.Received, 2017.
1001 Menichetti, L., Kätterer, T. and Leifeld, J.: Parametrization consequences of constraining soil
1002 organic matter models by total carbon and radiocarbon using long-term field data,
1003 Biogeosciences, 3003–3019, doi:10.5194/bg-13-3003-2016, 2016.
1004 Nash, J. E. and Sutcliffe, J. V: River flow forecasting through conceptual models part I — A
1005 discussion of principles, J. Hydrol., 10(3), 282–290, doi:https://doi.org/10.1016/0022-
1006 1694(70)90255-6, 1970.
1007 Ogle, K., Ryan, E., Dijkstra, F. A. and Pendall, E.: Journal of Geophysical Research:
1008 Biogeosciences, J. Geophys. Res. Biogeoscoences, 1–14, doi:10.1002/2016JG003385, 2016.
1009 Pappenberger, F. and Beven, K. J.: Ignorance is bliss: Or seven reasons not to use uncertainty
1010 analysis, Water Resour. Res., 42(5), doi:10.1029/2005WR004820, 2006.
1011 Peters, W., Jacobson, A. R., Sweeney, C., Andrews, A. E., Conway, T. J., Masarie, K., Miller, J.
1012 B., Bruhwiler, L. M. P., Pétron, G., Hirsch, A. I., Worthy, D. E. J., van der Werf, G. R.,
1013 Randerson, J. T., Wennberg, P. O., Krol, M. C. and Tans, P. P.: An atmospheric perspective
1014 on North American carbon dioxide exchange: CarbonTracker., Proc. Natl. Acad. Sci. U. S.
1015 A., 104(48), 18925–30, doi:10.1073/pnas.0708986104, 2007.

1016 Le Quéré, C., Peters, G. P., Andres, R. J., Andrew, R. M., Boden, T. A., Ciais, P., Friedlingstein,
1017 P., Houghton, R. A., Marland, G., Moriarty, R., Sitch, S., Tans, P., Arneth, A., Arvanitis, A.,
1018 Bakker, D. C. E., Bopp, L., Canadell, J. G., Chini, L. P., Doney, S. C., Harper, A., Harris, I.,
1019 House, J. I., Jain, A. K., Jones, S. D., Kato, E., Keeling, R. F., Klein Goldewijk, K.,
1020 Körtzinger, A., Koven, C., Lefèvre, N., Maignan, F., Omar, A., Ono, T., Park, G.-H., Pfeil,
1021 B., Poulter, B., Raupach, M. R., Regnier, P., Rödenbeck, C., Saito, S., Schwinger, J.,
1022 Segschneider, J., Stocker, B. D., Takahashi, T., Tilbrook, B., van Heuven, S., Viovy, N.,
1023 Wanninkhof, R., Wiltshire, A. and Zaehle, S.: Global carbon budget 2013, Earth Syst. Sci.
1024 Data, 6(1), 235–263, doi:10.5194/essd-6-235-2014, 2014.
1025 Raich, J. W. J. J. W., Potter, C. S. C. and Bhagawati, D.: Interannual variability in global soil
1026 respiration, 1980-94, Glob. Chang. Biol., 8, 800–812, doi:10.1046/j.1365-
1027 2486.2002.00511.x, 2002.
1028 Ren, X., He, H., Moore, D. J. P., Zhang, L., Liu, M., Li, F., Yu, G. and Wang, H.: Uncertainty
1029 analysis of modeled carbon and water fluxes in a subtropical coniferous plantation, J.
1030 Geophys. Res. Biogeosciences, 118(4), 1674–1688, doi:10.1002/2013JG002402, 2013.
1031 Ricciuto, D. M., King, A. W., Dragoni, D. and Post, W. M.: Parameter and prediction uncertainty
1032 in an optimized terrestrial carbon cycle model: Effects of constraining variables and data
1033 record length, J. Geophys. Res. Biogeosciences, 116(1), 1–17, doi:10.1029/2010JG001400,
1034 2011.
1035 Richardson, A. D. and Hollinger, D. Y.: Statistical modeling of ecosystem respiration using eddy
1036 covariance data: Maximum likelihood parameter estimation, and Monte Carlo simulation of
1037 model and parameter uncertainty, applied to three simple models, Agric. For. Meteorol.,
1038 131(3–4), 191–208, doi:10.1016/j.agrformet.2005.05.008, 2005.

1039 Sadegh, M. and Vrugt, J. A.: Bridging the gap between GLUE and formal statistical approaches:
1040 Approximate Bayesian computation, Hydrol. Earth Syst. Sci., 17(12), 4831–4850,
1041 doi:10.5194/hess-17-4831-2013, 2013.
1042 Scharnagl, B., Vrugt, J. A., Vereecken, H. and Herbst, M.: Inverse modelling of in situ soil water
1043 dynamics: Investigating the effect of different prior distributions of the soil hydraulic
1044 parameters, Hydrol. Earth Syst. Sci., 15(10), 3043–3059, doi:10.5194/hess-15-3043-2011,
1045 2011.
1046 Schimel, J. P. and Weintraub, M. N.: The implications of exoenzyme activity on microbial carbon
1047 and nitrogen limitation in soil: a theoretical model, Soil Biol. Biochem., 35(4), 549–563,
1048 doi:10.1016/S0038-0717(03)00015-4, 2003.
1049 Schmidt, M. W. I., Torn, M. S., Abiven, S., Dittmar, T., Guggenberger, G., Janssens, I. A., Kleber,
1050 M., Kögel-Knabner, I., Lehmann, J., Manning, D. A. C., Nannipieri, P., Rasse, D. P., Weiner,
1051 S. and Trumbore, S. E.: Persistence of soil organic matter as an ecosystem property, Nature,
1052 478(7367), 49–56, doi:10.1038/nature10386, 2011.
1053 Scholz, K., Hammerle, A., Hiltbrunner, E. and Wohlfahrt, G.: Analyzing the Effects of Growing
1054 Season Length on the Net Ecosystem Production of an Alpine Grassland Using Model – Data
1055 Fusion, Ecosystems, 21(5), 982–999, doi:10.1007/s10021-017-0201-5, 2018.
1056 Schoups, G. and Vrugt, J. A.: A formal likelihood function for parameter and predictive inference
1057 of hydrologic models with correlated, heteroscedastic, and non-Gaussian errors, Water
1058 Resour. Res., 46(10), 1–17, doi:10.1029/2009WR008933, 2010.
1059 Scott, R. L., Jenerette, G. D., Potts, D. L. and Huxman, T. E.: Effects of seasonal drought on net
1060 carbon dioxide exchange from a woody-plant-encroached semiarid grassland, J. Geophys.
1061 Res. Biogeosciences, 114(4), doi:10.1029/2008JG000900, 2009.

1062 Shi, X., Ye, M., Curtis, G. P., Miller, G. L., Meyer, P. D., Kohler, M., Yabusaki, S. and Wu, J.:
1063 Assessment of parametric uncertainty for groundwater reactive transport modeling, Water
1064 Resour. Res., 50(5), 4416–4439, doi:10.1002/2013WR013755, 2014.
1065 Sinsabaugh, R. L., Manzoni, S., Moorhead, D. L. and Richter, A.: Carbon use efficiency of
1066 microbial communities: stoichiometry, methodology and modelling, Ecol. Lett., 16(7), 930–
1067 939, doi:10.1111/ele.12113, 2013.
1068 Smith, M. W., Bracken, L. J. and Cox, N. J.: Toward a dynamic representation of hydrological
1069 connectivity at the hillslope scale in semiarid areas, Water Resour. Res., 46(12),
1070 doi:10.1029/2009WR008496, 2010a.
1071 Smith, T., Sharma, A., Marshall, L., Mehrotra, R. and Sisson, S.: Development of a formal
1072 likelihood function for improved Bayesian inference of ephemeral catchments, Water
1073 Resour. Res., 46(12), 1–11, doi:10.1029/2010WR009514, 2010b.
1074 Smith, T., Marshall, L. and Sharma, A.: Modeling residual hydrologic errors with Bayesian
1075 inference, J. Hydrol., 528, 29–37, doi:10.1016/j.jhydrol.2015.05.051, 2015.
1076 Spaaks, J. H. and Bouten, W.: Resolving structural errors in a spatially distributed hydrologic
1077 model using ensemble Kalman filter state updates, Hydrol. Earth Syst. Sci., 17(9), 3455–
1078 3472, doi:10.5194/hess-17-3455-2013, 2013.
1079 Steinacher, M. and Joos, F.: Transient Earth system responses to cumulative carbon dioxide
1080 emissions: Linearities, uncertainties, and probabilities in an observation-constrained model
1081 ensemble, Biogeosciences, 13(4), 1071–1103, doi:10.5194/bg-13-1071-2016, 2016.
1082 Tang, J. and Riley, W. J.: Weaker soil carbon–climate feedbacks resulting from microbial and
1083 abiotic interactions, Nat. Clim. Chang., 5, 56 [online] Available from:
1084 http://dx.doi.org/10.1038/nclimate2438, 2014.

1085 Tang, J. and Zhuang, Q.: A global sensitivity analysis and Bayesian inference framework for
1086 improving the parameter estimation and prediction of a process-based Terrestrial Ecosystem
1087 Model, J. Geophys. Res. Atmos., 114(D15), doi:10.1029/2009JD011724, 2009.
1088 Thiemann, M., Trosset, M., Gupta, H. and Sorooshian, S.: Bayesian recursive parameter estimation
1089 for hydrologic models, Water Resour. Res., 37(10), 2521–2535,
1090 doi:10.1029/2000WR900405, 2001.
1091 Thyer, M., Renard, B., Kavetski, D., Kuczera, G., Franks, S. W. and Srikanthan, S.: Critical
1092 evaluation of parameter consistency and predictive uncertainty in hydrological modeling: A
1093 case study using Bayesian total error analysis, Water Resour. Res., 45(12), 1–22,
1094 doi:10.1029/2008WR006825, 2009.
1095 Tiedeman, C. R. and Green, C. T.: Effect of correlated observation error on parameters,
1096 predictions, and uncertainty, Water Resour. Res., 49(10), 6339–6355,
1097 doi:10.1002/wrcr.20499, 2013.
1098 Tsai, F. T.-C. and Elshall, A. S.: Hierarchical Bayesian model averaging for hydrostratigraphic
1099 modeling: Uncertainty segregation and comparative evaluation, Water Resour. Res., 49(9),
1100 doi:10.1002/wrcr.20428, 2013.
1101 Tucker, C. L., Bell, J., Pendall, E. and Ogle, K.: Does declining carbon-use efficiency explain
1102 thermal acclimation of soil respiration with warming ?, Glob. Chang. Biol., 252–263,
1103 doi:10.1111/gcb.12036, 2013.
1104 Tucker, C. L., Young, J. M., Williams, D. G. and Ogle, K.: Process-based isotope partitioning of
1105 winter soil respiration in a subalpine ecosystem reveals importance of rhizospheric
1106 respiration, Biogeochemistry, 121, 389–408 [online] Available from:
1107 http://www.jstor.org/stable/24717586, 2014.

1108 Tuomi, M., Vanhala, P., Karhu, K., Fritze, H. and Liski, J.: Heterotrophic soil respiration-
1109 Comparison of different models describing its temperature dependence, Ecol. Modell.,
1110 211(1–2), 182–190, doi:10.1016/j.ecolmodel.2007.09.003, 2008.
1111 Vargas, R., Carbone, M. S., Reichstein, M. and Baldocchi, D. D.: Frontiers and challenges in soil
1112 respiration research: from measurements to model-data integration, Biogeochemistry,
1113 102(1), 1–13, doi:10.1007/s10533-010-9462-1, 2011.
1114 Vrugt, J. A. and Ter Braak, C. J. F.: DREAM(D): An adaptive Markov Chain Monte Carlo
1115 simulation algorithm to solve discrete, noncontinuous, and combinatorial posterior parameter
1116 estimation problems, Hydrol. Earth Syst. Sci., 15(12), 3701–3713, doi:10.5194/hess-15-
1117 3701-2011, 2011.
1118 Vrugt, J. A., ter Braak, C. J. F., Diks, C. G. H. and Schoups, G.: Hydrologic data assimilation using
1119 particle Markov chain Monte Carlo simulation: Theory, concepts and applications, Adv.
1120 Water Resour., 51, 457–478, doi:10.1016/j.advwatres.2012.04.002, 2013.
1121 Wang, G., Post, W. M. and Mayes, M. A.: Development of microbial-enzyme-mediated
1122 decomposition model parameters through steady-state and dynamic analyses, Ecol. Appl.,
1123 23(1), 255–272, doi:10.1890/12-0681.1, 2013.
1124 Weijs, S. V., Schoups, G. and Van De Giesen, N.: Why hydrological predictions should be
1125 evaluated using information theory, Hydrol. Earth Syst. Sci., 14(12), 2545–2558,
1126 doi:10.5194/hess-14-2545-2010, 2010.
1127 Westerberg, I. K., Guerrero, J. L., Younger, P. M., Beven, K. J., Seibert, J., Halldin, S., Freer, J.
1128 E. and Xu, C. Y.: Calibration of hydrological models using flow-duration curves, Hydrol.
1129 Earth Syst. Sci., 15(7), 2205–2227, doi:10.5194/hess-15-2205-2011, 2011.
1130 Wieder, W. R., Bonan, G. B. and Allison, S. D.: Global soil carbon projections are improved by

1131 modelling microbial processes, Nat. Clim. Chang., 3, 909 [online] Available from:
1132 http://dx.doi.org/10.1038/nclimate1951, 2013.
1133 Wieder, W. R., Allison, S. D., Davidson, E. A., Georgiou, K., Hararuk, O., He, Y., Hopkins, F.,
1134 Luo, Y., Smith, M. J., Sulman, B., Todd-Brown, K., Wang, Y.-P., Xia, J. and Xu, X.:
1135 Explicitly representing soil microbial processes in Earth system models, Global
1136 Biogeochem. Cycles, 29(10), 1782–1800, doi:10.1002/2015GB005188, 2015.
1137 Van Wijk, M. T., Van Putten, B., Hollinger, D. Y. and Richardson, A. D.: Comparison of different
1138 objective functions for parameterization of simple respiration models, J. Geophys. Res.
1139 Biogeosciences, 113(3), 1–11, doi:10.1029/2007JG000643, 2008.
1140 Xu, T., White, L., Hui, D. and Luo, Y.: Probabilistic inversion of a terrestrial ecosystem model:
1141 Analysis of uncertainty in parameter estimation and model prediction, Global Biogeochem.
1142 Cycles, 20(2), 1–15, doi:10.1029/2005GB002468, 2006.
1143 Xu, X., Schimel, J. P., Thornton, P. E., Song, X., Yuan, F. and Goswami, S.: Substrate and
1144 environmental controls on microbial assimilation of soil organic carbon: a framework for
1145 Earth system models, Ecol. Lett., 17(5), 547–555, doi:10.1111/ele.12254, 2014.
1146 Yeluripati, J. B., van Oijen, M., Wattenbach, M., Neftel, A., Ammann, A., Parton, W. J. and Smith,
1147 P.: Bayesian calibration as a tool for initialising the carbon pools of dynamic soil models,
1148 Soil Biol. Biochem., 41(12), 2579–2583, doi:10.1016/j.soilbio.2009.08.021, 2009.
1149 Yuan, W., Liang, S., Liu, S., Weng, E., Luo, Y. and Hollinger, D.: Improving model parameter
1150 estimation using coupling relationships between vegetation production and ecosystem
1151 respiration, Ecol. Modell., 240, 29–40, doi:10.1016/j.ecolmodel.2012.04.027, 2012.
1152 Yuan, W., Xu, W., Ma, M., Chen, S. and Liu, W.: Agricultural and Forest Meteorology Improved
1153 snow cover model in terrestrial ecosystem models over the Qinghai – Tibetan Plateau, Agric.

For. Meteorol., 218–219, 161–170, doi:10.1016/j.agrformet.2015.12.004, 2016.

Zhang, X., Niu, G.-Y., Elshall, A. S., Ye, M., Barron-Gafford, G. A. and Pavao-Zuckerman, M.: Assessing five evolving microbial enzyme models against field measurements from a semiarid savannah - What are the mechanisms of soil respiration pulses?, Geophys. Res. Lett., 41(18), doi:10.1002/2014GL061399, 2014.

Zhou, X., Luo, Y., Gao, C., Verburg, P. S. J., Arnone, J. A., Darrouzet-Nardi, A. and Schimel, D. S.: Concurrent and lagged impacts of an anomalously warm year on autotrophic and heterotrophic components of soil respiration: A deconvolution analysis, New Phytol., 187(1), 184–198, doi:10.1111/j.1469-8137.2010.03256.x, 2010.

Figure 1. Diagram of model 6C representing the processes of (1) degradation of soil organic carbon (SOC) to dissolved organic carbon (DOC) through catalysis of enzymes (ENZ) produced by microbes (MIC), (2) MIC uptake of DOC, and (3) microbial (MIC) respiration to produce CO_2 (CUE is the carbon use efficiency). SOC degradation and microbial uptake rates are controlled by water saturation (θ / θ_s). The DOC and ENZ pools are split into two subpools, one for the wet zone and the other for the dry zone of the soil pore space. Microbial uptake of DOC occurs only in the wet zone, and the uptake rate is linearly related to θ/θ_s. Catalysis through ENZ in the wet zone is proportional to θ/θ_s, while that in the dry zone is proportional to $1 - \theta/\theta_s$. V_{max} (s^{-1}) is the maximum rate, and K_m is the half-saturation concentration.

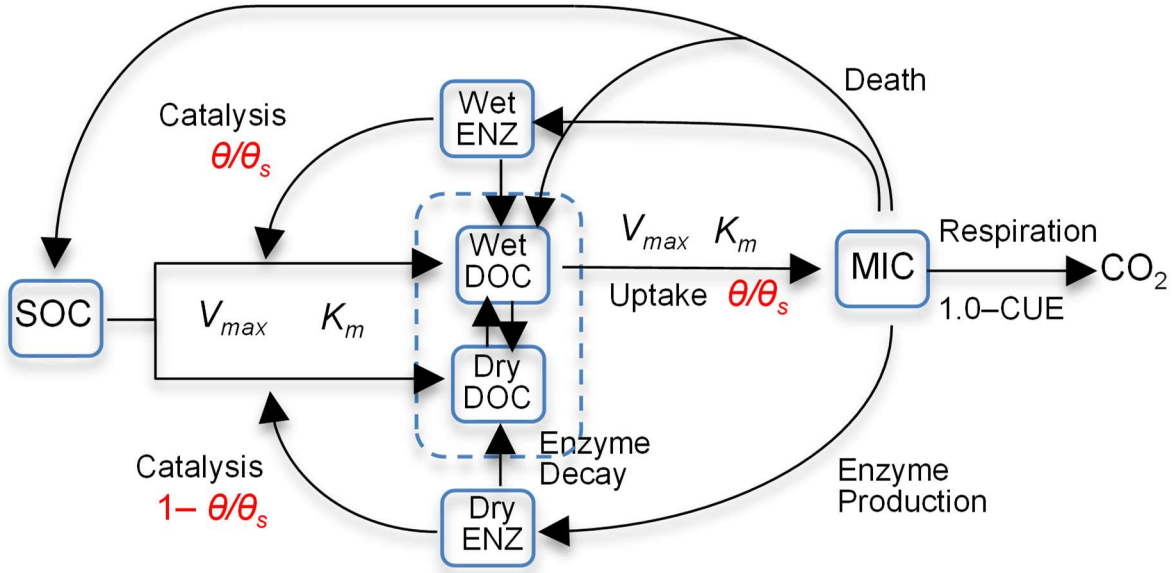

1176 Figure 2. Time series of soil moisture and efflux observations. The dashed line marks the divide
1177 of the dataset into calibration and validation periods.
1178

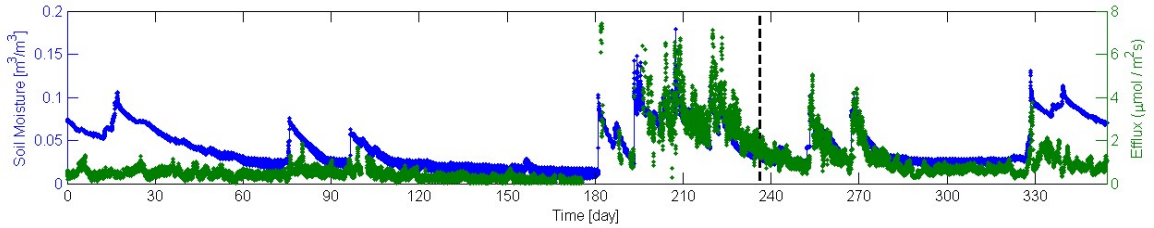

1179

Figure 3. Residual analysis of the best realization (among multiple MCMC realizations) for model 6C using data models (a-c) SLS and (d-f) WSEP-AC.

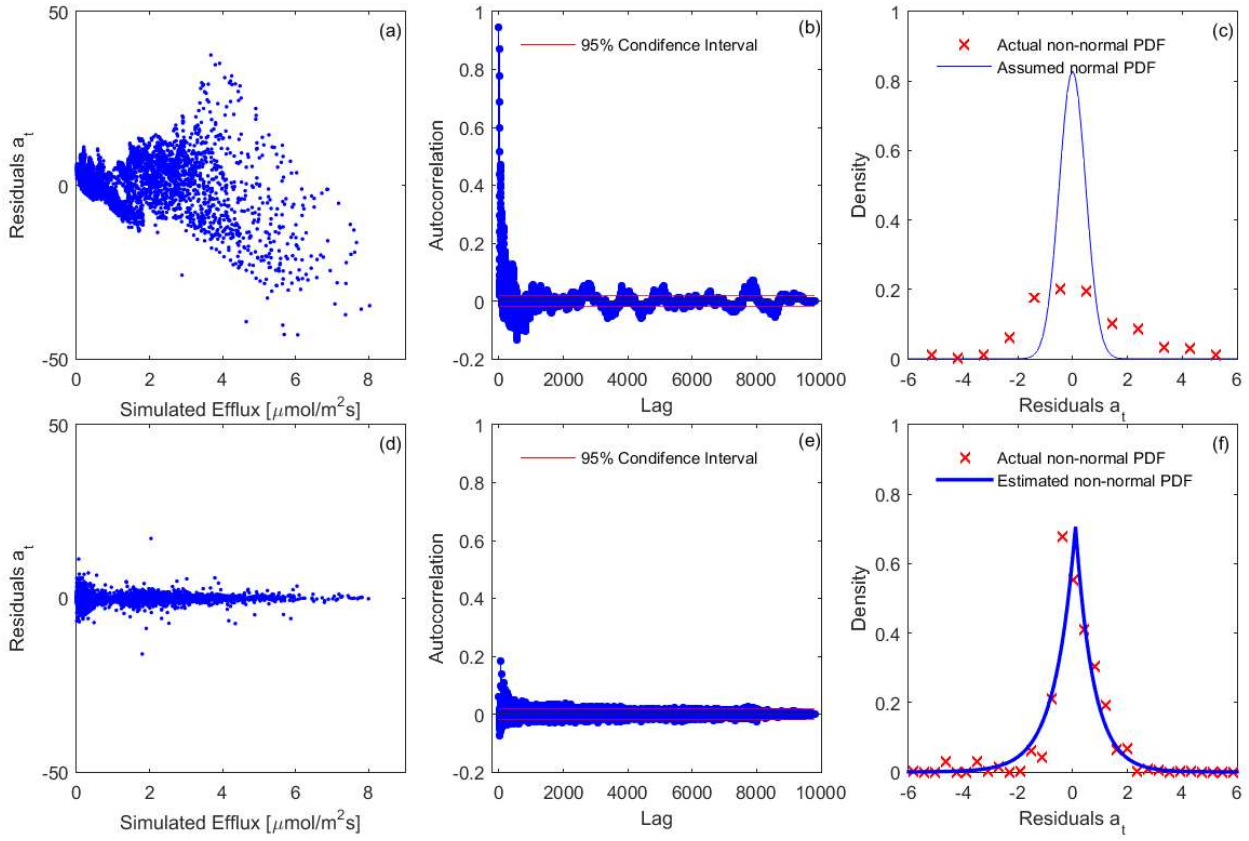

1184 Figure 4. Residual quantile-quantile (Q-Q) plots of the best realization (among multiple MCMC
1185 realizations) for the three soil respiration models and eight data models.
1186

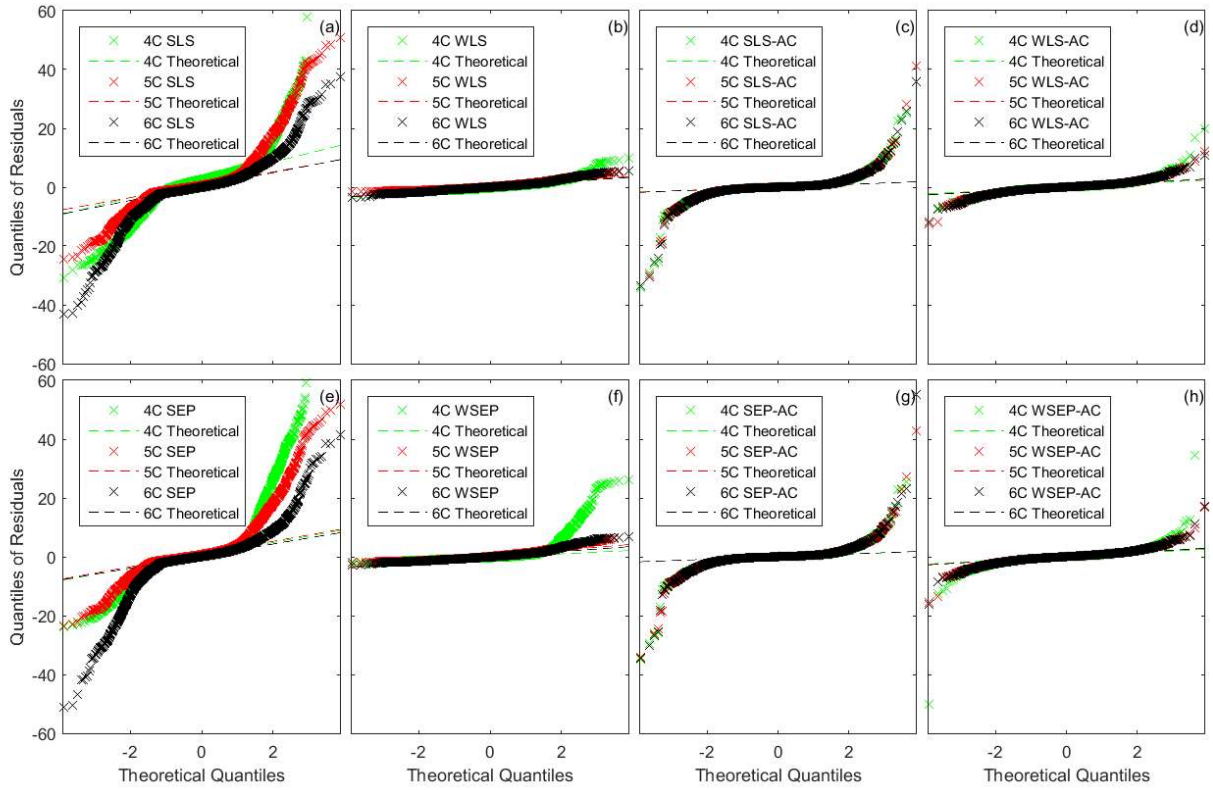

1187

Figure 5. Marginal posterior parameter density of carbon use efficiency (CUE) for the three soil respiration models and eight data models.

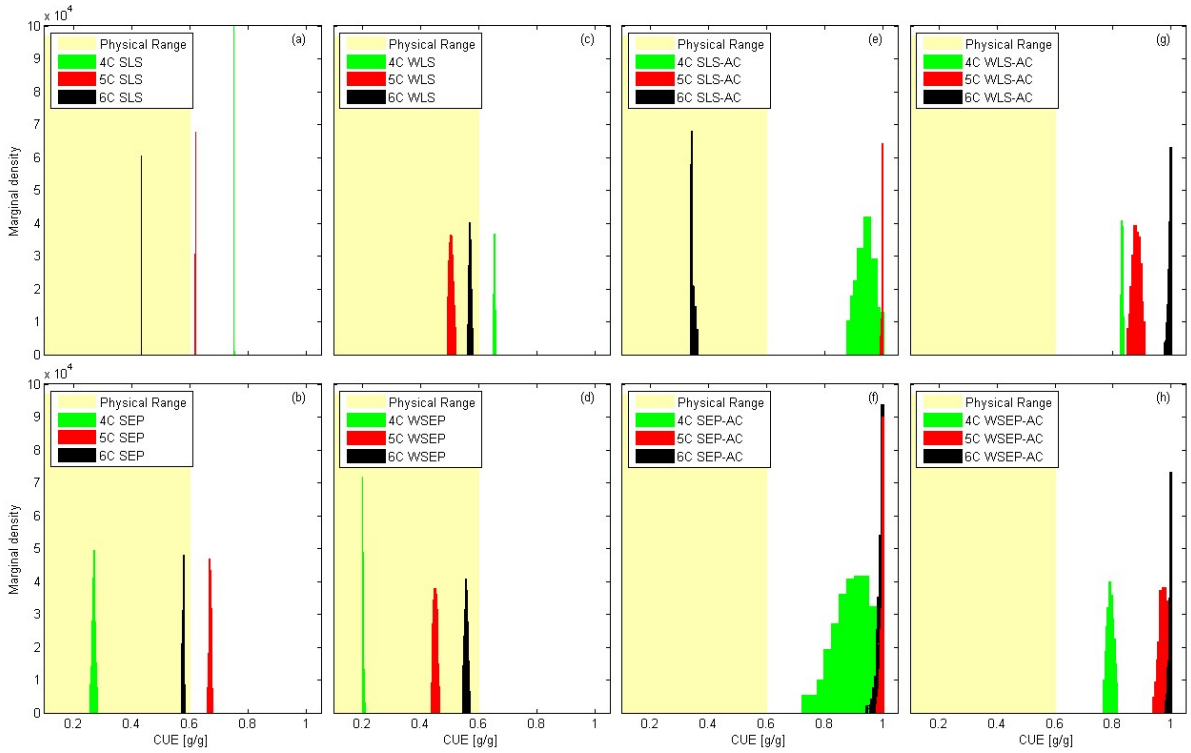

Figure 6. Observation data (blue dots) and mean prediction (green line) and 95% credible intervals (red line) of prediction ensembles for (a)-(f) the calibration period and (g)-(l) the validation period. The plots are for the three soil respiration models using data models SLS and WSEP-AC. *The prediction ensembles are generated to consider parametric uncertainty of the soil respiration models only.*

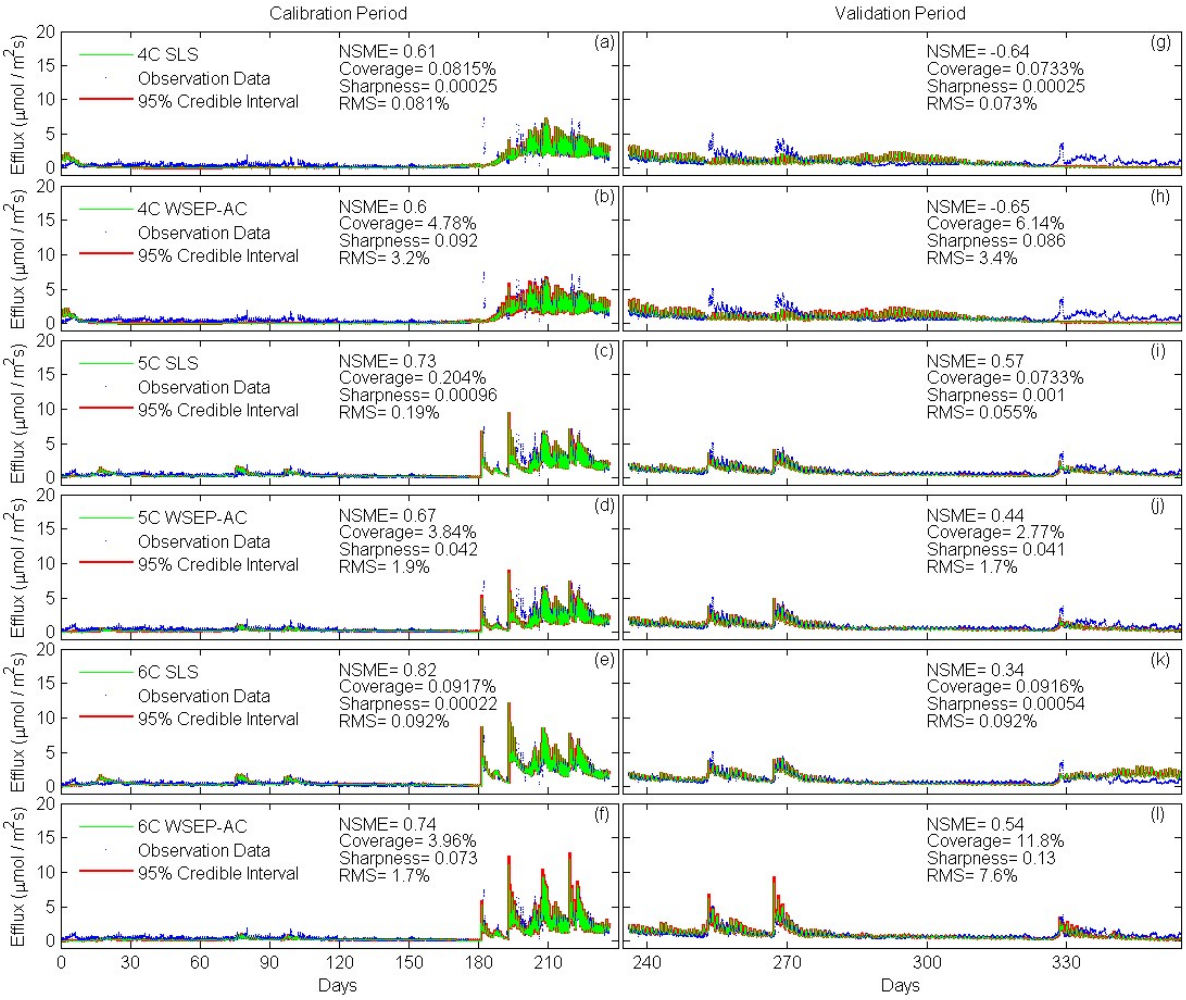

Figure 7. (a-b) Nash-Sutcliffe model efficiency (NSME), (c)-(d) sharpness, (e)-(f) predictive coverage, and (g)-(h) relative model score for measuring predictive performance of the three soil respiration models and the eight data models during the calibration and cross-validation periods. *The statistics are evaluated from the prediction ensembles generated to consider parametric uncertainty of the soil respiration models only.*

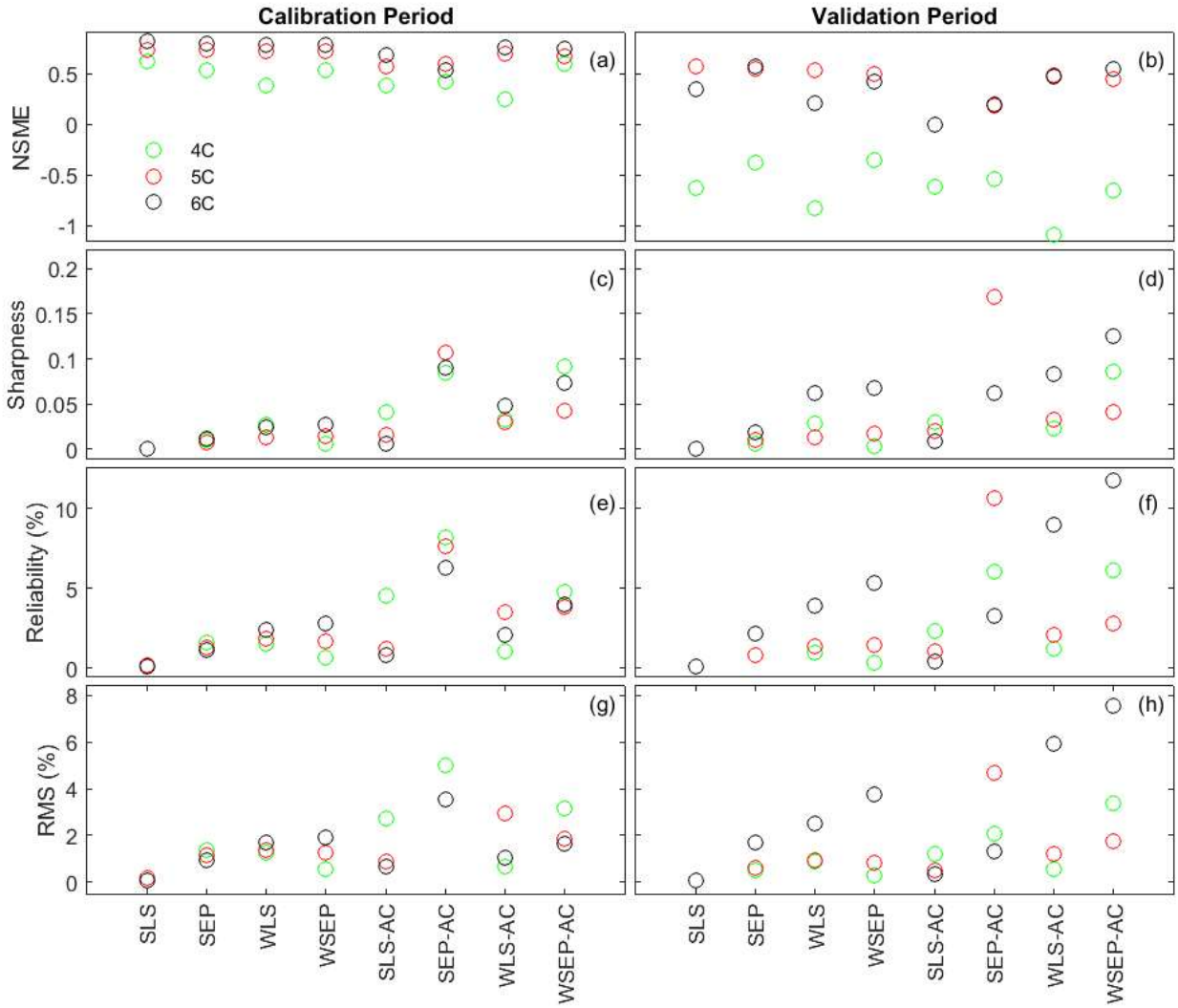

Figure 8. Observation data (blue dots) and mean prediction (green line) and 95% credible intervals (red line) of prediction ensembles for (a)-(f) the calibration period and (g)-(l) the validation period. The plots are for the three soil respiration models using data models SLS and WSEP-AC. *The prediction ensembles are generated to consider parametric uncertainty of not only the soil respiration models but also the data models.*

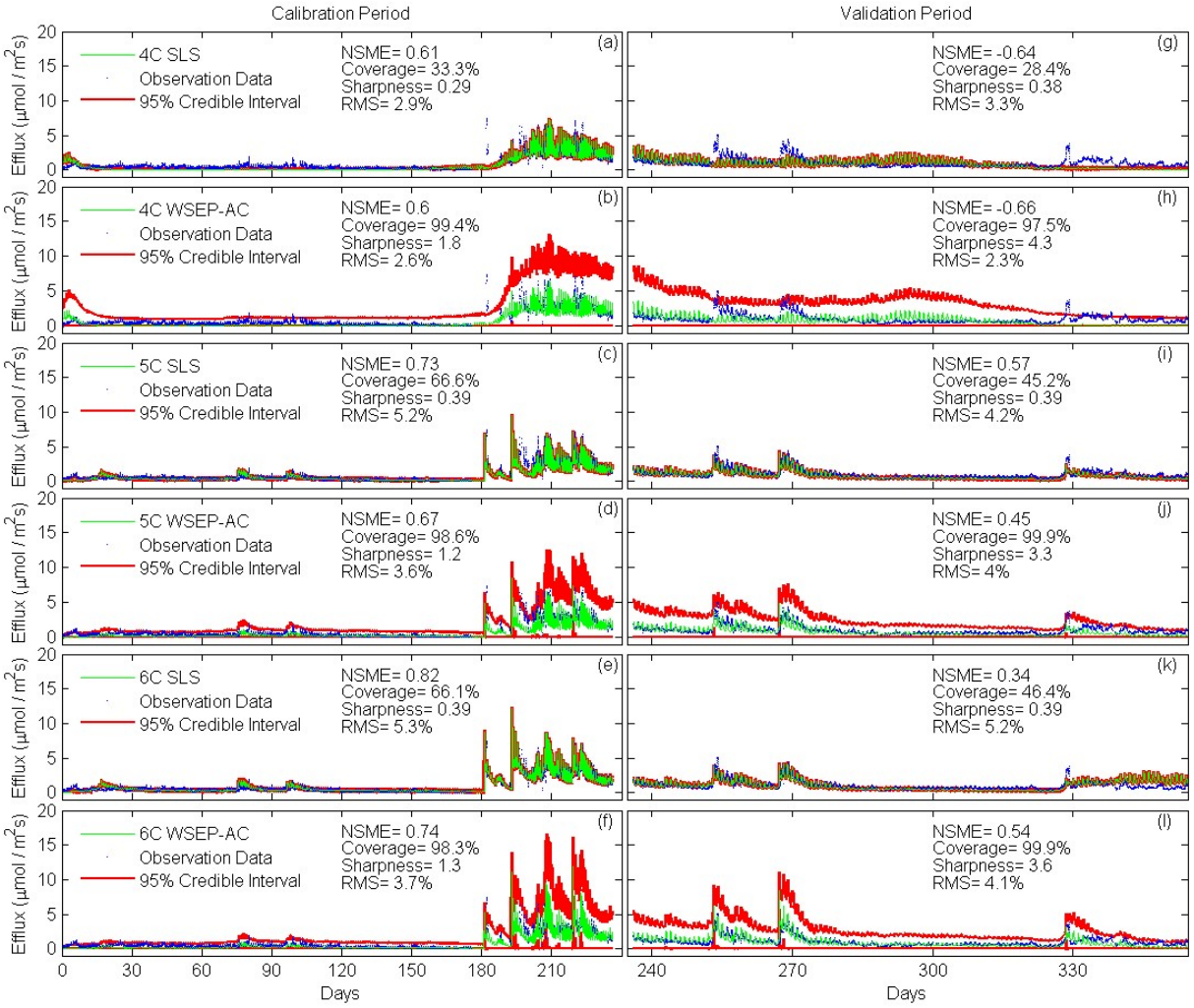

Figure 9. (a-b) Nash-Sutcliffe model efficiency (NSME), (c)-(d) sharpness, (e)-(f) predictive coverage, and (g)-(h) relative model score for measuring predictive performance of the three soil respiration models and the eight data models during the calibration and cross-validation periods. *The statistics are evaluated from the prediction ensembles generated to consider parametric uncertainty of not only the soil respiration models but also the data models.*

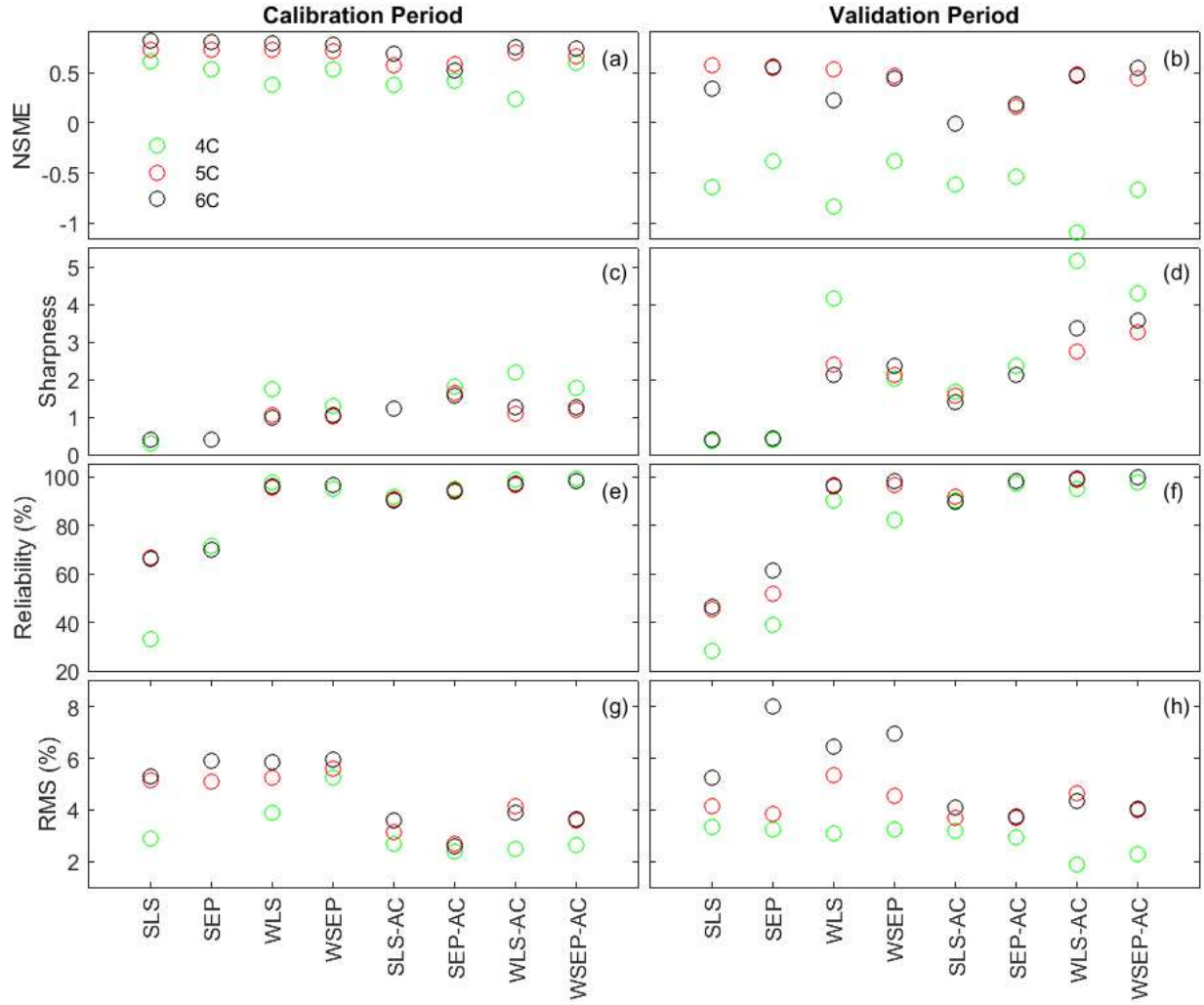

Figure 10. Observation data (blue dots) and mean prediction (green line) and 95% credible intervals (red line) for 6C for the eight likelihood functions during the calibration period (a)-(h) and the validation period (i)-(p). *The prediction ensembles are generated to consider parametric uncertainty of not only the soil respiration models but also the data models.*